AUT Journal of Electrical Engineering
10.22060/EEJ.2026.25913.6025

Integrated Energy Hub Optimization for Cost Reduction in a Fabric-Concrete Production Line Using Measurement-Based Modeling

Reza Rahmani[1], Reza Ghaffarpour[2,*]

[1]Department of Electrical Engineering, Amirkabir University of Technology (Tehran PolyTechnic), Tehran 1591634311, Iran

[2]Faculty of Energy Engineering, Imam Hossein University, Tehran, Iran

[*]Corresponding Author: rghaffarpour@ihu.ac.ir

Abstract

Industrial manufacturing lines are well suited to integrated multi-energy planning; however, many existing energy hub (EH) studies rely on synthetic load profiles or simplified thermal representations that limit their practical applicability at the factory scale. This paper develops a measurement-informed, factory-scale EH optimization model for a fabric-reinforced concrete production line. Grid electricity and natural gas are modeled as primary energy carriers, while photovoltaic (PV) generation, diesel backup generation, and furnace waste-heat recovery (WHR) are incorporated as complementary technologies within a transparent linear programming framework. All model parameters are derived from on-site electrical and thermal audit data, allowing the analysis to reflect the actual operating envelope of the production line. Seven scenarios are investigated to isolate the economic, environmental, and reliability impacts of PV self-consumption and export, diesel backup operation under grid outages, and WHR utilization. To assess the robustness of the proposed framework, sensitivity analyses are performed. Results indicate that under low industrial electricity tariffs, PV primarily contributes to emission reduction, whereas attractive feed-in tariffs transform PV into the most economically beneficial technology through electricity export. WHR consistently reduces natural gas consumption and associated emissions but remains economically attractive only under favorable fuel pricing or investment conditions. Diesel generation becomes economically justified only when grid outages and production losses are considered, highlighting its role as a resilience asset rather than a routine energy source. Overall, the proposed framework provides a transparent, computationally efficient, and policy-relevant decision-support tool for industrial EH planning under evolving market and regulatory conditions.

Keywords: Energy hub, Linear programming, Cost reduction, Waste-heat recovery, Measurement-based modeling.

1. Introduction

The construction sector is increasingly adopting advanced composite materials to address rising requirements for durability, lightweight design, and accelerated construction schedules. Among these materials, textile-reinforced (fabric-reinforced) concrete has emerged as a competitive alternative to conventional steel-reinforced concrete due to its high tensile capacity, corrosion resistance, and ability to enable thinner structural elements. These properties have driven its growing application in façade panels, prefabricated components, and modular construction systems, where production efficiency and material optimization are critical [1].

Despite these material-level advances, the industrial manufacturing of fabric-reinforced concrete remains energy-intensive. Fabric-concrete production lines typically rely on continuous operation of electrically driven equipment (such as conveying, deposition, and handling systems) coupled with hot-air furnaces for curing or thermal processing. The resulting energy demand profile is characterized by relatively steady electrical loads and a persistent thermal demand, leading to significant fuel consumption and exposure to energy price volatility. Moreover, hot-air furnaces continuously discharge exhaust gases at moderate temperatures, creating a non-negligible potential for waste-heat recovery (WHR) that is often left untapped in practice [2,3].

Improving energy efficiency and reducing operating costs in such facilities requires coordinated management of multiple energy carriers, including electricity, natural gas, and recoverable thermal energy. In this context, the energy-hub (EH) framework provides a unified modeling paradigm capable of representing heterogeneous energy sources, conversion technologies, and end-use demands within a single multi-carrier network. By explicitly capturing coupling relationships between electrical and thermal domains, EH models enable integrated optimization of energy flows under operational and balance constraints, making them particularly suitable for industrial systems with interdependent electric and thermal loads [4]. Recent developments in EH-based optimization have demonstrated the potential of integrated energy management to reduce costs and improve resource utilization in industrial environments [5]. However, most existing studies focus on generic manufacturing facilities, industrial microgrids, or hypothetical case studies, often relying on synthetic load profiles or simplified thermal representations. In contrast, fabric-reinforced concrete production lines present a distinct combination of features (continuous furnace operation, measurable exhaust heat streams, distributed motor loads, and increasing interest in on-site renewable generation) that have not yet been systematically analyzed within an EH framework. Furthermore, while advanced mixed-integer and stochastic optimization techniques have been widely explored, many industrial decision-makers prioritize transparency, computational efficiency, and direct applicability over model complexity. Linear programming (LP)-based formulations therefore remain highly attractive for factory-level planning studies, particularly when detailed field data are available and the primary objective is cost minimization under realistic operational constraints.

Motivated by these gaps, this study develops an integrated EH optimization model for a real-world fabric-reinforced concrete production line. Grid electricity and natural gas are considered as primary energy carriers, while photovoltaic (PV) generation, diesel backup generation, and furnace-based waste-heat recovery are evaluated as complementary options. Using measured plant-level data for electrical motors, furnace consumption, and operating schedules, the proposed LP framework minimizes the annualized total energy cost while satisfying all electrical and thermal balance constraints. The main contributions of this work are as follows:

(a) Development of a measurement-driven, factory-scale EH model tailored to a thermal-intensive fabric-reinforced concrete production line, demonstrating how LP-based formulations can provide actionable insights for industrial energy planning.

(b) Quantitative assessment of tariff- and policy-dependent technology roles, showing how industrial electricity prices and feed-in tariffs can fundamentally shift PV deployment from a self-consumption-oriented decarbonization option to a dominant cost-reduction asset via electricity export.

(c) Explicit characterization of reliability-oriented energy strategies, highlighting the conditions under which diesel backup generation becomes economically viable only when grid outages and production-loss penalties are explicitly accounted for, and identifying WHR as primarily an emission-driven option under low natural gas prices.

The remainder of this paper is organized as follows. Section 2 reviews recent literature on EH-based industrial optimization and waste-heat recovery. Section 3 describes the production line and data acquisition process. Section 4 presents the mathematical formulation and solution method. Section 5 discusses the numerical results and scenario analyses, and Section 6 concludes the paper and outlines directions for future research.

2. Literature Review and Research Gap

The literature concerning energy system optimization for industrial applications has evolved significantly, often paralleling advancements in computational mathematics and energy technology adoption. This section reviews the state-of-the-art in energy hub (EH) modeling, renewable integration, and waste heat recovery (WHR) within industrial optimization contexts, culminating in the clear articulation of the unique research gap addressed by this study.

2.1. Energy Hub Frameworks for Industrial Operation

The concept of the Energy Hub (EH) has been successfully adapted to manage the inherent complexity of industrial energy systems, which involve interdependent electricity, heat, and sometimes gas or cooling carriers [6, 7]. Early works often employed centralized optimization models, typically formulated as Mixed-Integer Linear Programs (MILP) [8], to ensure optimal dispatch by coordinating all assets under known deterministic forecasts. Building upon this centralized MILP paradigm, recent studies have extended the formulation to stochastic frameworks in order to capture renewable energy uncertainty and load flexibility; for instance, the stochastic MILP-based energy hub model proposed in [9] integrates ammonia as an energy carrier and employs scenario-based optimization to enhance operational robustness. More recently, the field has shifted toward distributed or multi-agent optimization schemes, which are favored for their scalability and robustness against communication failures, enabling local agents to make consensus-based decisions on energy transactions [10, 11]. Specifically in the context of industrial or regional energy management, frameworks like those proposed in [12] have emphasized resilience and maintenance scheduling, integrating these operational constraints directly into the MILP formulation to enhance supply reliability against component outages. While these sophisticated frameworks offer high accuracy, their reliance on high-dimensional MILP models can introduce significant computational overhead, making them less practical for time-sensitive, day-to-day operational planning in dynamic industrial environments [13].

2.2. Integration of Variable and Dispatchable Sources in EHs

The increasing penetration of variable renewable energy sources (VRES), such as Photovoltaic (PV) arrays, necessitates the integration of dispatchable backup units (e.g., diesel generators, boilers) and energy storage systems (ESS) within the EH structure [14]. Studies focusing on the economic dispatch of EHs under uncertainty (often driven by the stochastic nature of wind and solar power) have utilized advanced techniques like two-stage stochastic programming or robust optimization [15]. For instance, approaches incorporating hydrogen storage or advanced scheduling algorithms have been proposed to manage uncertainty effectively, often demonstrating substantial cost savings compared to deterministic methods [16, 17]. However, in many process industries where thermal demands are high and continuous, such as the curing stage in concrete production, the reliance on VRES is often limited by the need for constant heat supply, making the economic evaluation of hybrid systems that prioritize operating cost reduction (rather than just uncertainty mitigation) a key, yet often secondary, objective in the existing literature.

2.3. Waste Heat Recovery in Industrial Contexts

Waste Heat Recovery (WHR) is a well-established strategy for improving industrial energy efficiency, primarily implemented via heat exchangers like recuperators, regenerators, or Organic Rankine Cycles (ORC) [18]. The performance of these systems is often quantified by the Heat Recovery Effectiveness, typically ranging from 15% to over 80% depending on the technology and temperature grade [18, 19]. In the context of EHs, WHR is often modeled as an input source to supply the thermal demand or drive a heat pump. While studies on specific high-temperature applications, such as in the ceramics industry, have modeled ORC integration, the application of simpler, direct-contact technologies (like air-to-air recuperators for preheating combustion air) within a comprehensive system-level LP cost minimization framework remains less common [20]. Existing literature frequently analyzes WHR performance in isolation or uses complex models that do not translate easily to the operational constraints of standard factory floor energy management.

2.4. Positioning of the Current Study and Identified Gaps

Although recent Energy Hub research has made substantial progress in advanced optimization techniques, including stochastic programming, distributed optimization, and large-scale MILP formulations [13,17], comparatively less attention has been devoted to measurement-informed, factory-scale applications that directly support industrial operational decision-making using transparent and computationally efficient optimization models. Likewise, while waste heat recovery has been extensively investigated from thermodynamic and technology perspectives [18], its integration into practical factory-scale Energy Hub optimization remains relatively limited, particularly for continuous manufacturing processes with tightly coupled electrical and thermal demands. Against this background, several practical gaps can be identified in the existing literature. Specifically, relatively few studies simultaneously:

(a) utilize measured, non-aggregated operational data from an actual continuous curing furnace together with its associated electrical loads;
(b) employ a transparent Linear Programming (LP) formulation for operational cost minimization that can be readily implemented in industrial practice; and
(c) explicitly evaluate the techno-economic performance of direct air-to-air recuperative waste heat recovery integrated with photovoltaic generation and diesel backup within a unified Energy Hub framework.

Accordingly, this study develops a deterministic LP-based Energy Hub model parameterized using measured production-line characteristics obtained from a functioning textile-reinforced concrete manufacturing facility.

10.22060/EEJ.2026.25913.6025

Rather than proposing a new optimization methodology, the proposed framework demonstrates how a computationally efficient LP formulation can support practical industrial decision-making through integrated analysis of photovoltaic deployment, diesel backup operation, and direct waste heat recovery under realistic electricity and fuel tariff structures. The principal contribution of this work therefore lies in providing a measurement-informed, application-oriented Energy Hub framework that bridges the gap between advanced multi-energy optimization research and practical implementation for factory-scale industrial energy management.

3. Case Study Description and Data Acquisition

3.1. Overview of the Fabric-Concrete Production Line

The studied facility is a medium-scale fabric-concrete (textile-reinforced concrete) production line that operates in a continuous manner with sequential material handling, deposition, cement-based coating, and thermal bonding. Fig. 1 shows the production line. The main electrical loads include multiple induction motors installed along the production chain, such as initial fabric unwinding units, material deposition and conveying systems, intermediate storage stages, cutting and finishing equipment, and final roll-collection units. These motors operate under relatively steady conditions during production hours and constitute the dominant share of the electrical demand.

Thermal energy demand is primarily associated with hot-air furnaces used for drying and bonding processes. The furnaces operate continuously during production shifts (two 8-hour shifts per day) and are supplied by natural gas, with auxiliary electrical motors for air circulation and burner operation. Due to the continuous operation and elevated exhaust temperatures, the furnaces also represent a potential source of recoverable waste heat.

The continuous operation of both electrical drives and thermal furnaces, combined with limited load flexibility, makes the facility an appropriate candidate for integrated energy-hub optimization aimed at cost reduction and efficiency improvement.

Fig. 1. Fabric-concrete production line.

3.2. Electrical Load Characterization (Motors & Drives)

Electrical load data were obtained through detailed on-site measurements conducted during normal plant operation. This approach ensures that the optimization model reflects actual industrial operating conditions rather than nominal or assumed load profiles.

10.22060/EEJ.2026.25913.6025

The electrical demand of the production line consists of two main components: (a) electrically driven mechanical processes and (b) electrically assisted thermal processes associated with the furnaces.

The production line includes multiple induction motors responsible for:

- initial roll-unwinding and material positioning,
- conveyor motion across several stages,
- hopper drives for cement deposition,
- dosing and feed mechanisms,
- exhaust fan motors associated with furnace ventilation,
- end-of-line cutting and roll-up operations.

In addition to mechanical drives, the hot-air furnaces are equipped with auxiliary electrical subsystems, including blower motors, ignition units, and electric heating elements used for startup and preheating. These electrical heating components enable partial substitution of gas-based thermal input, particularly during furnace warm-up and load stabilization phases.

For each motor, the following data were recorded from nameplates and direct measurements:

- rated power (kW),
- nominal voltage and current,
- power factor,
- operating schedule,
- functional role within the production process.

All electrical loads (both mechanical and thermal auxiliaries) were aggregated into a unified electrical-demand vector used in the EH optimization model. Where real-time current data were required, measurements were conducted using clamp meters and portable load loggers in accordance with standard industrial energy-auditing practices.

3.3. Thermal Load Characterization (Hybrid Gas–Electric Furnace System)

The production line includes two gas-fired hot-air furnaces responsible for supplying process heat at temperatures up to approximately 250 °C. Both furnaces operate in parallel during production hours, with a typical daily operating duration of 16 hours. Unlike a purely fuel-based representation, the furnaces are modeled as hybrid thermal units capable of receiving energy from multiple sources. The primary thermal input is provided through natural gas combustion, while auxiliary electric heating elements support furnace startup, preheating, and partial thermal supply. Accordingly, only a limited fraction of the total thermal demand can be supplied electrically. This configuration reflects common industrial practice and introduces an explicit coupling between electrical and thermal energy carriers.

According to manufacturer specifications and verified through direct on-site observations, the main technical characteristics of each furnace are as follows:

- **Natural gas consumption** ≈ 15 m^3/h,
- **Blower motor**: 5.5 kW (continuous operation),
- **Ignition/auxiliary motor**: 0.55 kW.
- **Electric heating elements**: 24 kW.

For modeling and optimization purposes, the two furnaces are treated as an aggregated thermal load with a total nominal gas consumption of approximately 30 m^3/h during steady operation. The associated electrical consumption of furnace auxiliaries and electric heating elements is included in the overall electrical demand of the plant.

Due to continuous operation and elevated exhaust gas temperatures, the furnaces provide a suitable opportunity for waste-heat recovery (WHR). Accordingly, WHR integration is considered as an optional technology within the EH optimization framework. The associated parameters, including heat-recovery efficiency, capital investment, and operation and maintenance (O&M) costs, are adopted from representative WHR studies and industrial practice and are detailed in the model formulation section.

3.4. Measurement Procedure and Instrumentation

Data acquisition followed a structured methodology to ensure accuracy and compatibility with the optimization model. The following instrumentation was used:

- **Clamp-meter (digital)** for measuring current, power factor, and real power of motors.
- **Digital gas flow meter** for estimating instantaneous and hourly gas consumption (validated by manufacturer data).
- **Thermocouples** for measuring furnace inlet/outlet temperatures, enabling preliminary WHR potential estimation.
- **Multi-channel datalogger** for capturing temporal variability of key electrical loads.
- **Facility utility invoices** to obtain representative electricity and natural-gas tariff ranges.

All measurements were conducted in coordination with plant technical staff to ensure safe access to electrical panels and gas facilities.

3.5. Energy Carriers Considered in the EH Model

In the current production configuration, the facility is supplied by grid electricity and natural gas. For optimization purposes, additional on-site energy options are considered, including photovoltaic (PV) generation and diesel-based backup generation. Furthermore, the continuous operation of the furnaces creates an opportunity for integrating waste-heat recovery through a heat-exchanger system, enabling partial reuse of exhaust thermal energy within the plant.

The system boundary is therefore defined to include multiple energy carriers (electricity and natural gas), conversion units, and end-use demands, consistent with the EH paradigm.

The EH model incorporates grid electricity and natural gas as primary energy carriers, while photovoltaic generation, a diesel generator, and a furnace-integrated waste-heat recovery unit are considered as candidate on-site technologies. Each component is represented within the EH framework through energy balance equations, capacity constraints, efficiency parameters, and operating schedule.

The EH structure of the industrial production line is shown in Fig. 2.

10.22060/EEJ.2026.25913.6025

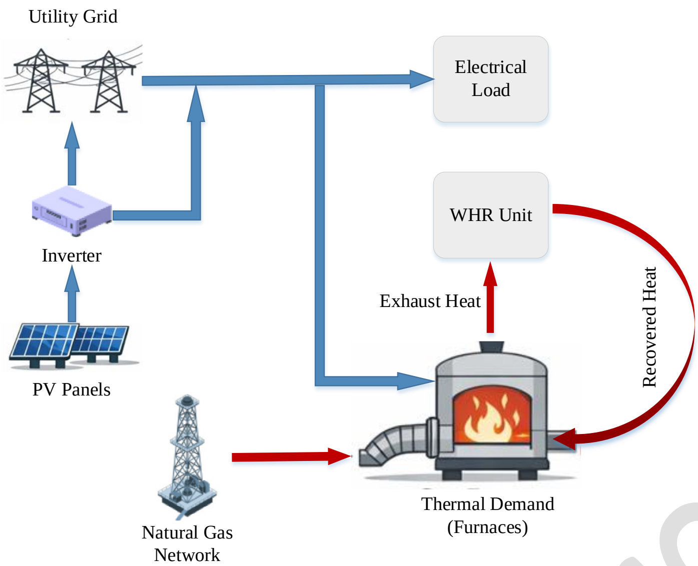

Fig. 2. Conceptual EH structure

3.6. Summary of Collected Parameters

The collected electrical, thermal, economic, and operational data were consolidated into a structured dataset for model formulation. Table 1 summarizes the key parameter categories, their main attributes, and corresponding data sources. This systematic data organization enhances model transparency and reproducibility.

Table 1. Summary of measured and collected parameters used in the EH optimization model

Category	Parameter	value	Source
Electrical motors	- Rated power Recorded per motor (aggregate) - Power factor (PF) - Voltage - duty cycle	- 111.42 kW - 0.78-0.85 - 400 V - 16 h/day	Nameplate + clamp-meter measurements
Furnace thermal demand	- Number of furnaces - Gas consumption - operating temperature - duty cycle	- 2 units - 2×15 m³/h - Up to 250 °C - 16 h/day	Manufacturer specifications + on-site observation
Tariffs	- Electricity tariff - gas tariff -PV feed-in tariff	- 9,982 IRR/kWh - 11,762 IRR/m³ - 31,500 IRR/kWh	Utility invoices/ national tariff tables
WHR potential	- Exhaust gas temperature - Technology - Indicative efficiency range - WHR capacity	- measured, > 180 °C - recuperative burner - 60–70 % [18] - Derived in optimization model	Thermocouple measurement + WHR / industrial heat-exchanger literature
Solar resource	- Global horizontal irradiance (GHI) - PV capacity - PV derating factors	- site specific annual profile - Derived in optimization model - 0.75-0.8	Meteonorm / national meteorology
Diesel generator	- Fuel cost - minimum loading - Diesel generator rated capacity (kW)	- 35,000 IRR/kWh - 30-40% - Derived in optimization model	Literature + datasheet+ local data
Operating schedule	- Shift duration - Daily production hours	- 2 shifts × 8 h - 16 h/day	Plant operational logs

	- Annual working days	- 240 days/year	

Based on the aggregated motor ratings and operating schedules, the total installed electrical capacity is approximately 111 kW. However, the average power demand during operation is around 90 kW. Under a typical operating regime of 16 h/day and 240 working days per year, the annual electricity consumption is estimated at approximately 345 MWh/year. Fig. 3 shows the collected data.

The thermal demand is dominated by gas-fired hot-air furnaces, with a measured natural gas consumption of approximately 15 m³/h per furnace and a typical daily operating duration of 16 hours.

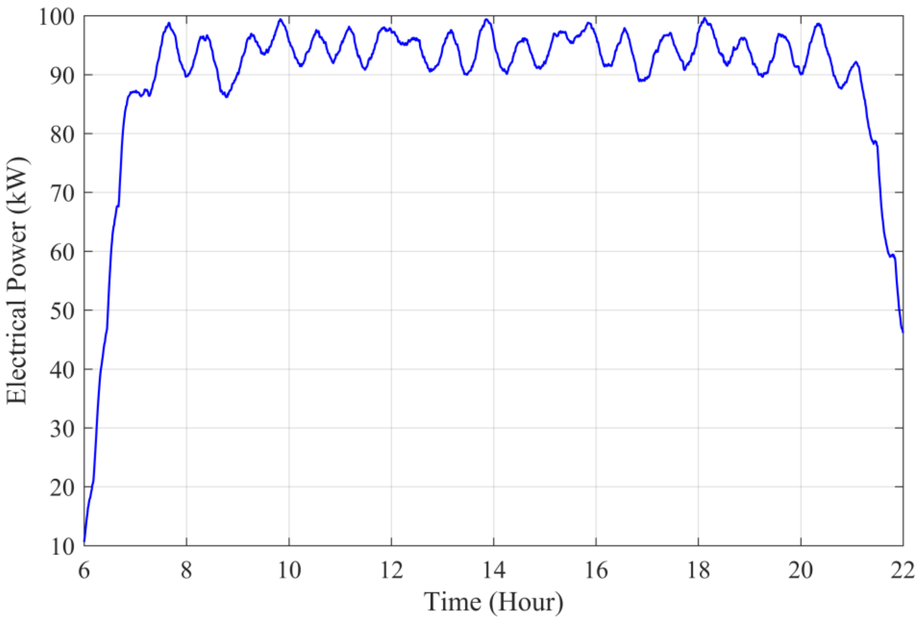

Fig. 3. Electrical load profile

3.7. Modeling Scope and Assumptions for Optimization

Photovoltaic generation is considered as a candidate on-site energy source to reduce electricity procurement from the grid. Importantly, the maximum installable PV capacity is constrained by the available roof or land area rather than by the instantaneous electrical demand of the factory. Accordingly, the PV capacity is bounded by a physical area-based limit, while operational interaction with the grid allows for both electricity import and export.

In addition to self-consumption, surplus PV electricity may be exported to the grid under existing feed-in or guaranteed purchase schemes. This enables the production facility to operate as a prosumer, where excess generation contributes to revenue and offsets total energy costs. The economic impact of grid export is explicitly modeled in the objective function and evaluated through scenario analysis, while regulatory and technical limits on export capacity are represented through appropriate constraints.

At this stage, the aggregated electrical and thermal demands are treated as fixed inputs to the optimization problem. The EH model focuses on minimizing the total annualized energy cost while satisfying energy balance relations, capacity limits, and operational constraints. Detailed dynamic behavior, such as transient motor loading or short-term thermal fluctuations, is outside the scope of the present study and left for future extensions. Accordingly, the proposed model is formulated as a deterministic linear programming problem focused on long-term operational cost minimization rather than short-term dynamic control.

10.22060/EEJ.2026.25913.6025

The proposed Energy Hub model was parameterized using operational information collected from the investigated factory, including installed motor capacities, furnace characteristics, equipment efficiencies, production schedules, and actual operating hours. The electrical demand profile was estimated from the rated capacities of production equipment together with the recorded daily operating schedule, while the thermal demand was calculated according to the measured furnace specifications and fuel characteristics. The photovoltaic generation system and waste heat recovery unit represent future investment alternatives evaluated within the optimization framework rather than existing plant assets. Consequently, the optimization results should be interpreted as a techno-economic assessment of prospective energy system configurations based on actual factory operating conditions instead of a retrospective reproduction of historical plant operation.

4. Mathematical Formulation of the EH Model

This section presents the mathematical formulation of the proposed energy hub (EH) model developed for optimal energy cost minimization in a fabric-concrete production line. The formulation follows the canonical EH modeling structure widely adopted in high-impact energy journals, ensuring clarity, transparency, and reproducibility [1-3]. The resulting optimization problem is formulated as a deterministic LP model, which is particularly suitable for factory-scale decision support where robustness and computational efficiency are prioritized over model complexity [9,10].

Before presenting the mathematical formulation, the principal decision variables and model parameters employed throughout the optimization model are summarized in Table 2. These symbols are used consistently in the subsequent equations to improve the readability and reproducibility of the proposed Energy Hub formulation.

Table 2. Nomenclature of the proposed Energy Hub model

Symbol	Description	Unit
Decision Variables		
P_t^{grid}	Electricity purchased from the utility grid at time (t)	kW
P_{rated}^{PV}	Photovoltaic system rated power	kW
P_t^{diesel}	Diesel generator output power at time (t)	kW
G_t	Natural gas consumption of the furnace at time (t)	m³
Parameters		
$P_t^{PV,sell}$	Electrical power exported by the PV at time (t)	kW
P_t^{Load}	Electrical demand at time (t)	kW
Q_t^{Load}	Thermal demand at time (t)	kW
$P^{elec}{}_{Q,t}$	Electrical consumption of heating elements at time t	kW
c_t^{grid}	Electricity purchase tariff	IRR/kWh
c_t^{gas}	Natural gas price	IRR/m³
C_{fuel}^{diesel}	Diesel generation cost	IRR/kWh
c_t^{sell}	PV feed-in tariff	IRR/kWh
LHV	Lower heating value of natural gas	kWh/m³
$\eta^{furnace}$	Furnace thermal efficiency	–
η^{WHR}	Waste heat recovery effectiveness	–
P_{max}^{PV}	Maximum installable PV capacity	kW
$P^{P\bar{V}}$	Installed PV capacity	kW
$P^{diesel,max}$	Maximum diesel generator capacity	kW
Q_t^{gas}	thermal energy supplied by natural gas	kWh
$Q_t^{furnace,max}$	Maximum thermal capacity of the furnace	kWh
Q_t^{elec}	Thermal energy supplied via electric heating	kWh
$Q_t^{exhaust}$	Available exhaust thermal energy	kWh
α_{max}	Maximum feasible electric heating share	–
CRF	Capital recovery factor	–
r	Discount rate	–
N	System life time	year
α_t	Solar availability factor at time t ($\in[0,1]$)	–

4.1. EH Structure and Modeling Scope

The considered energy hub integrates multiple energy carriers and conversion technologies within a unified optimization framework. Electricity and natural gas are treated as primary energy inputs, while photovoltaic (PV) generation, a diesel generator (DG), and furnace-based WHR are incorporated as on-site resources. Electrical energy is used to supply motor-driven equipment along the production line, whereas thermal energy is mainly required by continuous hot-air furnaces and can be supplied through a hybrid configuration consisting of natural gas combustion and auxiliary electric heating. Waste heat from furnace exhaust gases is recovered through a recuperative air-to-air heat exchanger, which directly preheats combustion air and reduces fuel consumption. This WHR configuration is consistent with established industrial practice for medium-temperature exhaust streams and has been widely reported in the literature [11,12]. The EH operates on an hourly basis over a representative operating horizon, capturing the steady and continuous nature of both electrical and thermal demands in the studied production line.

4.2. Modeling Assumptions

To maintain computational efficiency while preserving the essential operational characteristics of the investigated industrial Energy Hub, the following assumptions are adopted throughout the optimization framework:

1. The scheduling horizon is divided into discrete hourly time intervals, and steady-state operation is assumed within each interval.
2. Electrical and thermal demands are considered deterministic and are estimated from the actual production schedule, installed equipment capacities, and operating hours obtained from the investigated production line.
3. The PV system and WHR unit are treated as candidate technologies for future implementation. Accordingly, their performance is evaluated through techno-economic optimization rather than historical operational measurements.
4. The thermal efficiency of the natural gas furnace is assumed constant throughout the scheduling horizon.
5. The waste heat recovery unit is modeled as a direct air-to-air recuperator with constant recovery effectiveness, neglecting transient thermal dynamics and heat losses within the ducting system.
6. Electrical transmission losses and thermal distribution losses inside the production facility are assumed negligible due to the relatively short internal distribution distances.
7. The lower heating value (LHV) of natural gas is assumed constant during the scheduling period.
8. Equipment operating limits, including maximum grid import capacity, PV generation capacity, diesel generator capacity, and natural gas consumption, are represented by linear constraints.
9. Energy storage systems and demand response programs are not considered in the present study, allowing the proposed formulation to focus on evaluating the techno-economic interactions among grid electricity, photovoltaic generation, diesel backup generation, natural gas consumption, and waste heat recovery.

4.3. Objective Function: Total Annualized Energy Cost Minimization

The objective of the proposed EH model is to minimize the total annualized energy cost of the fabric-concrete production line while satisfying all electrical and thermal demands and operational constraints.

The total cost consists of four main components:

1. Cost of electricity purchased from the grid
2. Fuel cost associated with diesel generation and natural gas consumption
3. Annualized investment cost of photovoltaic (PV), diesel generation and WHR installation
4. Operation and maintenance (O&M) costs of on-site generation units
5. Revenue from selling surplus PV electricity to the grid (if applicable)

The objective of the proposed EH model is to minimize the total annualized energy cost, consisting of: a) operational expenditures (OPEX), b) annualized capital investment costs (CAPEX) and c) operation and maintenance costs (O&M), as commonly adopted in EH-based industrial optimization studies:

$$OF = C_{\text{OPEX}} + C_{\text{CAPEX,ann}} + C_{\text{O\&M}} - R_{\text{PV,Sell}} \tag{1}$$

Where each term is defined as follows.

4.3.1. Operational Cost (OPEX)

The operational cost includes electricity purchases from the grid, natural gas consumption by furnaces, and diesel fuel consumption:

$$C_{\mathrm{OPEX}} = \sum_{t \in T} \left(c_t^{\mathrm{grid}} P_t^{\mathrm{grid}} + c_t^{\mathrm{gas}} G_t + c_{\mathrm{fuel}}^{\mathrm{diesel}} P_t^{\mathrm{diesel}} \right) \Delta t \tag{2}$$

Where,

- c_t^{grid} is the electricity tariff at time t and P_t^{grid} is the power purchased from the grid (kW).
- c_t^{gas} is the unit price of natural gas and G_t is gas consumption of the furnaces (m^3).
- $c_{\mathrm{fuel}}^{\mathrm{diesel}}$ and P_t^{diesel} represent the unit cost of diesel fuel and diesel electricity output, respectively.
- Δt is the duration of each time step (h).

4.3.2. Annualized Capital Cost (CAPEX)

Capital investments for PV, diesel generator, and waste-heat recovery systems are converted into equivalent annual costs using the capital recovery factor (CRF):

$$C_{\mathrm{CAPEX,ann}} = \sum_{i \in \{PV, WHR, diesel\}} C_{\mathrm{CAPEX}}^{i} . CRF \tag{3}$$

Where, CRF is the capital recovery factor, defined as:

$$CRF = \frac{r(1+r)^N}{(1+r)^N - 1} \tag{4}$$

with r being the discount rate and N the system lifetime (years).

4.3.3. Operation and Maintenance Costs

The O&M cost accounts for routine maintenance and operational expenses of on-site technologies. These costs are modeled as proportional to installed capacity or energy output, following standard industrial practice [9,13,14].

$$C_{\mathrm{O\&M}} = C_{\mathrm{O\&M}}^{\mathrm{PV}} + C_{\mathrm{O\&M}}^{\mathrm{diesel}} + C_{\mathrm{O\&M}}^{\mathrm{WHR}} \tag{5}$$

The individual O&M components are defined as:

$$C_{\mathrm{O\&M}}^{\mathrm{PV}} = c_{\mathrm{O\&M}}^{\mathrm{PV}} \times P_{\mathrm{rated}}^{\mathrm{PV}} \tag{6}$$

$$C_{\mathrm{O\&M}}^{\mathrm{diesel}} = c_{\mathrm{O\&M}}^{\mathrm{diesel}} \times P_t^{\mathrm{diesel}} \tag{7}$$

$$C_{\mathrm{O\&M}}^{\mathrm{WHR}} = c_{\mathrm{O\&M}}^{\mathrm{WHR}} \times Q_{\mathrm{rated}}^{\mathrm{WHR}} \tag{8}$$

where $c_{O\&M}^{(.)}$ denotes the unit O&M cost of each technology.

10.22060/EEJ.2026.25913.6025

4.3.4. Revenue from Selling Excess PV Electricity

If grid regulations allow selling surplus PV electricity, the corresponding revenue is modeled as:

$$R_{\mathrm{PV,Sell}} = \sum_{t \in T} c_t^{\mathrm{sell}} P_t^{\mathrm{PV,sell}} \Delta t \tag{9}$$

Where, c_t^{sell} and $P_t^{\mathrm{PV,sell}}$ are the feed-in tariff and the exported PV power at time t, respectively.

4.3.5. Discussion

Because all cost coefficients remain constant throughout each scheduling interval and all system constraints are formulated as linear relationships, the resulting optimization problem constitutes a LP model that can be solved efficiently using standard optimization algorithms. This linear formulation provides a transparent and computationally efficient framework suitable for industrial day-ahead operational planning while maintaining sufficient modeling accuracy for techno-economic assessment. The proposed objective function integrates both operational and investment costs within a unified linear structure. This formulation enables the assessment of trade-offs between grid dependency, on-site renewable generation, diesel backup usage, and thermal energy utilization. Moreover, incorporating PV export revenue allows the model to capture the economic potential of over-sizing PV capacity under favorable feed-in tariffs, which is particularly relevant in regions with guaranteed power purchase schemes.

4.4. Energy Balance Constraints

In an EH framework, system feasibility is ensured by enforcing energy balance constraints for each energy carrier. In the proposed model, two primary carriers are considered: electricity and thermal energy. These balances must be satisfied at every time step to guarantee reliable operation of the production line.

4.4.1. Electrical Power Balance

At each time step t, the total electrical demand of the production line must be met by the available electricity supply sources, including grid electricity, on-site PV generation, and diesel generation.

$$P_t^{\mathrm{grid}} + P_t^{\mathrm{PV}} + P_t^{\mathrm{diesel}} = P_t^{\mathrm{Load}} + P_t^{\mathrm{PV,sell}} \qquad \forall t \in T \tag{10}$$

This formulation explicitly allows PV generation to either supply internal loads or be exported to the grid, depending on economic conditions and feed-in tariffs.

4.4.2. Electrical Load Representation

The electrical demand of the production line is modeled as the aggregated power consumption of all motor-driven equipment:

$$P_t^{\mathrm{Load}} = \sum_{i \in M} P_{t,i} + P_{\mathrm{Q},t}^{\mathrm{elec}} \tag{11}$$

Where, $P_{t,i}$ is the active power consumption of motor i at time t and M denotes the set of electrical motors and equipment. $P^{\mathrm{elec}}_{\mathrm{Q},t}$ is the electrical consumption of heating elements at time t.

Given the relatively stable operating conditions of the production line, the load is assumed to be deterministic within each operating shift. This assumption is consistent with prior industrial EH studies focused on factory-scale systems.

10.22060/EEJ.2026.25913.6025

4.4.3. Thermal Energy Balance

Thermal energy demand is primarily associated with the hot-air furnaces used in the fabric-concrete production process. The thermal balance is expressed as:

$$Q_t^{\mathrm{gas}} + Q_t^{\mathrm{elec}} + Q_t^{\mathrm{WHR}} = Q_t^{\mathrm{Load}} \qquad \forall t \in T \tag{12}$$

$$Q_t^{\mathrm{elec}} = P_{\mathrm{Q},t}^{\mathrm{elec}} \times \eta_{\mathrm{elec}}^{\mathrm{furnace}} \qquad \forall t \in T \tag{13}$$

Where,

- Q_t^{gas}: thermal energy supplied by natural gas combustion.
- Q_t^{elec}: thermal energy supplied via electric heating.
- Q_t^{WHR}: recovered thermal energy from furnace exhaust gases.
- Q_t^{load}: thermal demand of the furnaces.

4.4.4. Waste-Heat Recovery Modeling

In thermal-intensive production lines, a considerable portion of the input fuel energy is discharged as waste heat through furnace exhaust gases. In the studied fabric-concrete production line, the hot-air furnace operates continuously for long periods at relatively steady temperatures, making it a suitable candidate for WHR. Integrating WHR into the EH allows part of this otherwise lost thermal energy to be reused, thereby reducing natural gas consumption and overall energy cost. The recoverable thermal energy from furnace exhaust gases is modeled as a fraction of the input fuel energy:

$$Q_t^{\mathrm{WHR,max}} = \eta^{\mathrm{WHR}} Q_t^{\mathrm{exhaust}} \tag{14}$$

Where, η^{WHR} and Q_t^{exhaust} represent the heat recovery efficiency and the available exhaust thermal energy, respectively.

For simplicity and tractability, Q_t^{exhaust} is assumed proportional to the natural gas input:

$$Q_t^{\mathrm{exhaust}} = \left(1 - \eta^{\mathrm{furnace}}\right) Q_t^{\mathrm{gas}} \tag{15}$$

Where, η^{furnace} is the thermal efficiency of the furnace.

The recovered heat contributes directly to meeting the thermal demand of the production process and reduces the required fuel input to the furnace. Accordingly, the natural gas consumption can be expressed as:

$$G_t = \frac{Q_t^{\mathrm{Load}} - Q_t^{\mathrm{WHR}} - Q_t^{\mathrm{elec}}}{\eta^{\mathrm{furnace}}.\mathrm{LHV}} \tag{16}$$

Where, LHV is the lower heating value of natural gas.

From an economic perspective, recovered waste heat is assumed to have zero fuel cost. However, the investment and maintenance costs associated with the heat recovery unit must be accounted for. These costs are incorporated into the objective function through an annualized capital cost and a fixed O&M cost. This formulation ensures that WHR affects the optimization in two complementary ways: (a) indirectly, by reducing natural gas consumption through the thermal balance constraints, and (b) directly, by introducing additional capital and maintenance costs into the objective function.

10.22060/EEJ.2026.25913.6025

The proposed formulation preserves the first-law energy balance while maintaining linearity, thereby enabling the optimization problem to be solved efficiently using LP techniques. Although detailed thermodynamic phenomena such as variable exhaust gas temperature, transient furnace dynamics, pressure losses, and heat exchanger fouling are neglected, the adopted formulation provides an appropriate level of fidelity for plant-level techno-economic planning studies in which operational scheduling rather than detailed thermal equipment design constitutes the primary objective.

4.4.5. Discussion

The energy balance constraints ensure that electrical and thermal demands are met at all times while explicitly capturing the coupling between fuel input, waste-heat recovery, and energy utilization. By separating electrical and thermal balances and linking them through WHR relations, the model maintains a clear physical interpretation and remains suitable for linear programming-based optimization. This structure also enables straightforward extension to additional carriers or technologies in future studies.

4.5. Operational Constraints of EH Components

The operation of each component within the proposed EH is constrained by physical capacity limits, availability profiles, and practical operating considerations. These constraints ensure that the optimization results remain technically feasible and directly applicable to the real production facility.

4.5.1. Grid Electricity Exchange Constraints

Electricity exchanged with the utility grid is bounded by the maximum aggregated electrical consumptions:

$$0 \le P_t^{\mathrm{grid}} \le P_t^{\mathrm{Load}} \qquad \forall t \in T \qquad (17)$$

In addition, exported PV electricity is limited by grid interconnection rules:

$$0 \le P_t^{\mathrm{PV,sell}} \le P^{\mathrm{sell,max}} \qquad \forall t \in T \qquad (18)$$

Where, $P^{\mathrm{sell,max}}$ is the maximum export capacity defined by feed-in regulations.

4.5.2. Photovoltaic (PV) Generation Constraints

PV generation at time t is constrained by the installed capacity and the normalized solar availability profile:

$$0 \le P_t^{\mathrm{PV}} \le P^{\bar{\mathrm{PV}}} \alpha_t \qquad \forall t \in T \qquad (19)$$

Where, $P^{\bar{\mathrm{PV}}}$ is the installed PV capacity and $\alpha_t \in [0,1]$ is the solar availability factor at time t.

The installed PV capacity itself is limited by the available installation area:

$$0 \le P^{\bar{\mathrm{PV}}} \le P^{\mathrm{PV,max}} \qquad (20)$$

Where, $P^{\mathrm{PV,max}}$ is derived from the available land or rooftop area and module power density.

4.5.3. Diesel Generator Operating Constraints

The diesel generator is modeled as a dispatchable backup source subject to capacity limits:

10.22060/EEJ.2026.25913.6025

$$0 \le P_t^{\text{diesel}} \le P^{\text{diesel,max}} \qquad \forall t \in T \tag{21}$$

Given the operational role of the diesel generator as a supplementary source, minimum up/down time constraints are neglected to preserve linearity, which is consistent with factory-scale EH models focused on economic dispatch.

4.5.4. Natural Gas Supply and Furnace Constraints

The thermal output of the gas-fired furnace is bounded by its rated capacity:

$$0 \le Q_t^{\text{gas}} \le Q_t^{\text{furnace,max}} \qquad \forall t \in T \tag{22}$$

This constraint ensures that the thermal demand of the hot-air furnace remains within safe operating limits.

$$0 \le Q_t^{\text{glec}} \le \alpha_{\max} Q_t^{load} \qquad \forall t \in T \tag{23}$$

Where, $\alpha_{\max}$ is maximum feasible electric heating share.

4.5.5. Waste-Heat Recovery Constraints

Recoverable thermal energy is limited by the availability of exhaust heat and the technical recovery efficiency:

$$0 \le Q_t^{\text{WHR}} \le Q_t^{\text{WHR,max}} \qquad \forall t \in T \tag{24}$$

Where, Q_t^{WHR} is calculated from (14).

This formulation guarantees that waste-heat recovery does not exceed physically available thermal energy and remains proportional to furnace operation.

4.5.6. Discussion

These operational constraints reflect real-world technical limitations of industrial energy systems while preserving a linear structure suitable for LP optimization. The explicit inclusion of PV capacity limits, grid exchange bounds, and waste-heat recovery constraints ensures that the model captures both physical feasibility and regulatory considerations relevant to industrial energy planning.

4.6. Optimization Algorithm and Solution Strategy

The formulated EH optimization problem aims to minimize the total annual energy supply cost while satisfying electrical and thermal balance constraints, operational limits of energy carriers and technology-specific restrictions. Given the linear structure of the objective function and constraints at the current stage, the problem is initially formulated as a LP model.

The LP formulation enables efficient solution of large-scale, time-resolved problems and provides a transparent benchmark for evaluating the economic performance of different energy supply options. Decision variables include grid electricity import and export, natural gas consumption, photovoltaic (PV) generation utilization, diesel generator output, and recovered waste heat. All costs (energy tariffs, fuel prices, and annualized investment and O&M costs) are incorporated consistently within the objective function.

The optimization problem is solved over a discretized time horizon T using a deterministic approach, assuming known demand profiles and tariff structures. This choice is justified by the relatively stable operating conditions of the production line and the objective of identifying cost-optimal energy supply configurations under typical operating scenarios.

4.7. Model Assumptions, Scope, and Limitations

The proposed optimization framework is formulated as a deterministic LP problem in which both the objective function and all governing constraints are linear. Consequently, the feasible solution space is convex, ensuring convergence toward the global optimum without dependence on initial values. The model is solved using MATLAB® linprog with the interior-point algorithm, which is well suited for large-scale linear optimization problems due to its computational efficiency and numerical robustness.

The primary motivation for adopting a deterministic LP formulation is threefold. First, industrial manufacturing plants generally perform production planning based on predetermined production schedules and contractual energy tariffs, allowing relatively accurate estimation of short-term electrical and thermal demands. Second, deterministic LP provides globally optimal solutions with very low computational effort, making it highly suitable for practical industrial energy management systems that require rapid and transparent operational decisions. Third, the linear structure facilitates straightforward interpretation of the contribution of each energy source and technology to the overall operating cost, thereby improving the practical applicability of the proposed framework for industrial decision-makers.

Nevertheless, the proposed formulation has several limitations that should be acknowledged. The model does not explicitly represent uncertainties associated with photovoltaic generation, future electricity market prices, natural gas price fluctuations, equipment outages, or unexpected production disturbances. These uncertainties may influence the optimal dispatch strategy, particularly under highly volatile market conditions or high renewable penetration. Moreover, the current model assumes perfect knowledge of system parameters and does not consider forecast errors or probabilistic operating conditions.

Despite these limitations, deterministic optimization remains an appropriate choice for the investigated industrial application. The production process considered in this study operates under relatively stable manufacturing schedules and continuous thermal demand, while the economic evaluation primarily focuses on comparing different technology deployment scenarios using identical operating conditions. Consequently, the deterministic formulation enables a transparent assessment of the relative economic benefits of PV generation and WHR without introducing additional uncertainty-related modeling complexity that could obscure the underlying techno-economic insights. Therefore, this work prioritizes industrial applicability, computational transparency, and direct implementation using measured operational data from an existing production line. The combination of field-calibrated data, explicit furnace-level WHR integration, and a computationally efficient LP framework provides an appropriate balance between modeling fidelity and practical deployability for day-ahead industrial energy management

Future research may extend the proposed framework by incorporating stochastic programming, robust optimization, or distributionally robust optimization to explicitly address renewable generation uncertainty, energy price volatility, demand uncertainty, equipment reliability, and carbon pricing policies. Such extensions would further improve the applicability of the framework under increasingly dynamic and uncertain industrial energy markets.

5. Results and Discussion

5.1. Baseline Energy Cost and Load Characteristics (Scenario S1)

Prior to introducing alternative energy supply options, a baseline scenario (S1) is defined in which the fabric-concrete production line is fully supplied by grid electricity and natural gas. This configuration represents the current operating practice of the plant and serves as the reference case for all subsequent scenarios. Based on measured motor ratings and actual operating schedules, the electrical demand exhibits relatively steady consumption during production hours, with limited short-term variability. This behavior is mainly attributed to the continuous operation of conveying, cutting, and forming equipment. Similarly, the hot-air furnaces operate for extended periods under quasi-constant thermal load, reflecting the continuous nature of the drying and curing process. Such load characteristics indicate low operational flexibility but high suitability for efficiency-oriented solutions, such as photovoltaic power generation and waste heat recovery.

As summarized in Table 3, the baseline annual energy cost is dominated by electricity purchased from the grid (5.3×10^9 IRR/year) and natural gas consumption in the furnaces (1.53×10^9 IRR/year), resulting in a total annual expenditure of approximately 6.82×10^9 IRR/year. Although both electricity and natural gas contribute to the total energy expenditure, electricity clearly dominates the cost structure, accounting for nearly 78% of the annual energy cost. This dominance is driven by the high cumulative electrical demand of motor-driven processes and the increased sensitivity of total operating cost to electricity tariff variations. As a result, the baseline configuration is particularly exposed to fluctuations in electricity prices, underscoring the economic relevance of electricity-oriented optimization strategies in subsequent scenarios. In this baseline configuration, no on-site generation, storage, or waste-heat recovery systems are employed, leaving the plant fully exposed to external energy prices and lacking operational flexibility.

The associated environmental impact is quantified using standard emission factors for grid electricity and natural gas. A carbon intensity of 0.93 kg CO_2/kWh is adopted for grid electricity [17], while natural gas combustion emissions are calculated using the IPCC guideline value of 2.1 kg CO_2/m³ [21]. As reported in Table 1, the baseline operation results in approximately 766 t CO_2/year, with electricity consumption accounting for the largest share of total emissions. This emission level represents an upper-bound benchmark against which the environmental benefits of PV integration, diesel backup, and waste-heat recovery are evaluated in subsequent scenarios.

Table 3. Baseline Energy Cost and Consumption Summary (Scenario S1)

Parameter	Value	Unit
Annual electricity cost	5,296,149,740	IRR/year
Annual thermal energy cost (natural gas)	1,526,739,970	IRR/year
Total annual energy cost	**6,822,889,710**	**IRR/year**
Share of electricity cost	77.6	%
Share of thermal energy cost	22.4	%
Annual Grid electricity purchased	530,570	kWh/year
Annual electricity consumption by motors	345,600	kWh/year
Annual electricity consumption by furnaces	184,970	kWh/year
Annual natural gas consumption	129,803	m³/year
Dominant cost carrier	Electricity	-
On-site generation	None	-
Energy export	None	-
CO_2 from electricity	493,430	kg CO_2/year
CO_2 from natural gas	272,586	kg CO_2/year
Total CO_2 emissions estimate	**766,016**	**kg CO_2/year**

5.2. Impact of Photovoltaic Integration

5.2.1. Photovoltaic Self-Consumption Scenario (Scenario S2)

In Scenario S2, photovoltaic (PV) generation is introduced as an on-site electricity supply option while maintaining grid electricity as the complementary source. In this configuration, no electricity export to the grid is allowed, and all PV generation is restricted to self-consumption within the plant. This scenario aims to evaluate the techno-economic and environmental impacts of partial renewable integration under the existing tariff structure, without relying on policy-driven incentives or feed-in mechanisms.

Based on the optimization results, the optimal installed PV capacity is determined as 153 kW, constrained by the available installation area and the self-consumption requirement. The annual electrical energy demand of the production line remains unchanged relative to Scenario S1 (530,570 kWh/year), which includes both motor loads

10.22060/EEJ.2026.25913.6025

and the electrically supplied share of furnace heating. Under this configuration, the PV system generates approximately 251,280 kWh/year, supplying 47.4% of the total electrical demand, while the remaining 129,240 kWh/year is imported from the grid (As shown in Table 4). From an operational perspective, PV generation supplies both motor-driven equipment (216,360 kWh/year) and part of the electrically assisted furnace heating (34,920 kWh/year). As a consequence, the electrically supplied thermal share of the furnace increases, which leads to a higher reliance on natural gas for meeting the remaining thermal demand. Accordingly, annual natural gas consumption rises from 129,803 m^3/year in the baseline case to 145,598 m^3/year, resulting in a corresponding increase in thermal energy cost. Economically, the integration of PV under self-consumption conditions yields a moderate reduction in total annual energy cost. Grid electricity expenditure decreases substantially from 5.30×10^9 IRR/year to 1.29×10^9 IRR/year. However, this reduction is partially offset by the annualized PV investment and operation cost (2.13×10^9 IRR/year) and the increased natural gas cost (1.71×10^9 IRR/year). As a result, the total annual energy cost decreases from 6.82×10^9 IRR/year in Scenario S1 to 5.13×10^9 IRR/year in Scenario S2, corresponding to an overall cost reduction of approximately 24.8%.

Despite the limited economic benefit, Scenario S2 delivers a pronounced environmental improvement. Since PV electricity is assumed to have zero operational CO_2 emissions, the reduction in grid electricity consumption leads to a substantial decrease in electricity-related emissions from 493,430 kg CO_2/year in the baseline case to 120,193 kg CO_2/year. Although natural-gas-related emissions increase slightly due to higher fuel consumption (305,756 kg CO_2/year), the net plant-level emissions are reduced to 425,949 kg CO_2/year, representing a total CO_2 reduction of 44.4% relative to Scenario S1.

Overall, Scenario S2 demonstrates that PV self-consumption in fabric-concrete production lines primarily functions as an effective decarbonization strategy rather than a strong cost-minimization measure under current industrial electricity tariffs. This finding aligns with recent industrial EH studies, which emphasize that the economic attractiveness of PV systems is highly sensitive to tariff structures and electricity export policies. The hourly average contribution of energy sources for Scenario S2 is illustrated in Fig. 3.

Table 4. Comparison of baseline operation and PV-integrated scenario (S2)

Parameter	S1: Baseline	S2: Grid + PV
PV rated capacity (kW)	0	153
Annual grid electricity (kWh/year)	530,570	129,240
Annual electricity consumption by motors provided by grid (kWh/year)	345,600	129,240
Annual electricity consumption by furnaces provided by grid (kWh/year)	184,970	0
Annual electricity consumption by motors provided by PV (kWh/year)	0	216,360
Annual electricity consumption by furnaces provided by PV (kWh/year)	0	34,920
Annual PV generation (kWh/year)	0	251,280
PV share	0%	47.36%
Annual natural gas consumption (m^3/year)	129,803	145,598
Annual thermal energy cost (natural gas)	1.53×10^9	1.71×10^9
Annual grid electricity cost (IRR/year)	5.3×10^9	1.29×10^9
Annualized PV cost (IRR/year)	0	2.13×10^9
Total annual energy cost (IRR/year)	6.82×10^9	5.13×10^9
CO_2 from electricity (kg CO_2/year)	493,430	120,193
CO_2 from natural gas (kg CO_2/year)	272,586	305,756
Total CO_2 emissions (kg CO_2/year)	766,016	425,949
CO_2 reduction vs. S1	-	44.39%

10.22060/EEJ.2026.25913.6025

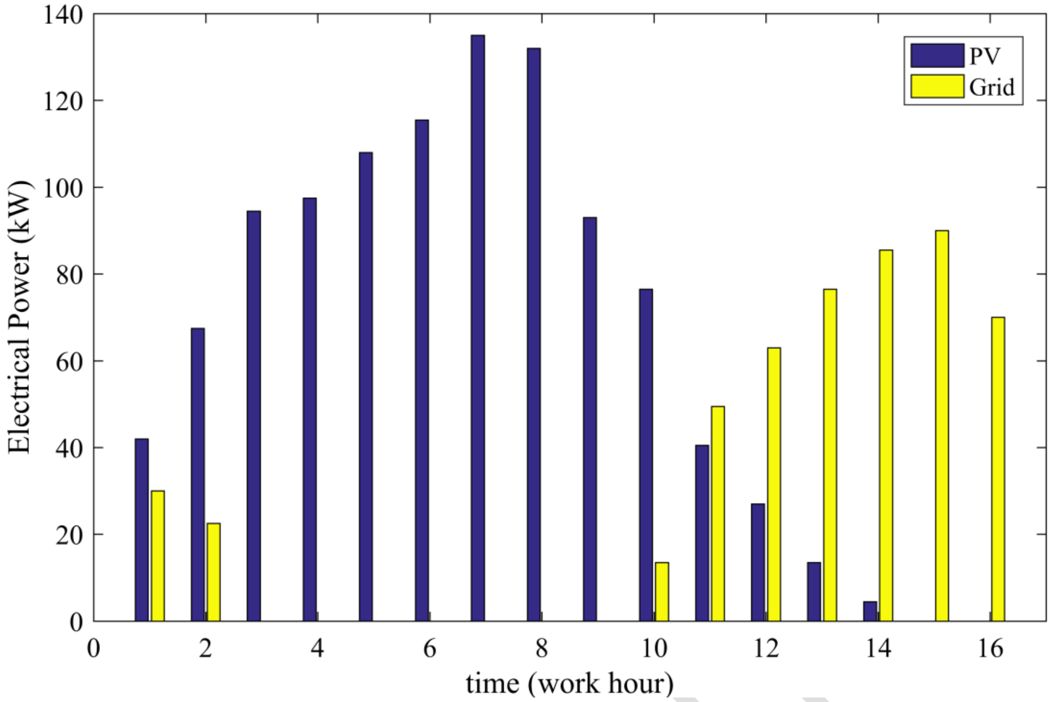

Fig. 3. Electrical power balance in scenario S2

5.3. Grid-Connected Photovoltaic System with Electricity Export (Scenario S3)

Scenario S3 investigates the impact of allowing full electricity export from an on-site photovoltaic (PV) system under a guaranteed feed-in tariff scheme. In contrast to Scenario S2 (where PV generation is limited to partial self-consumption) this configuration permits PV installation up to the maximum capacity allowed by available land area, independent of the plant's internal electrical demand. Such a setting reflects current renewable energy support mechanisms, in which surplus solar electricity can be sold to the grid at a fixed tariff substantially higher than the industrial electricity purchase price.

5.3.1. Optimal Capacity Selection and Energy Flows

In this scenario, an important operational shift occurs in the thermal subsystem. Given the relatively low cost of natural gas compared with industrial electricity tariffs, all process heat required by the hot-air furnaces is supplied exclusively by natural gas. Electrically assisted heating is therefore fully eliminated. As a result, the electrical demand of the plant consists solely of motor-driven equipment, while thermal demand is entirely decoupled from electricity consumption.

Consequently, the entire electrical load of the production line is supplied by grid electricity, whereas all PV-generated electricity is exported to the grid. This configuration reflects a rational cost-minimization strategy in the presence of a strong price asymmetry between electricity purchase tariffs, gas tariffs, and PV feed-in incentives.

Based on the available land area, the maximum installable PV capacity is limited to 250 kW. Optimization results indicate that this upper bound is fully utilized. The annual PV electricity generation reaches approximately 401,500 kWh/year, all of which is exported to the grid. Since electrically supplied heating is removed, the annual grid electricity consumption is reduced relative to Scenario S1 and corresponds only to motor-driven loads. Meanwhile, natural gas consumption increases moderately compared with PV self-consumption scenarios, as all thermal demand is now met by gas-fired furnaces.

This outcome highlights a key feature of integrated energy-hub optimization: when multiple energy carriers are available, the model naturally reallocates demand toward the most cost-effective carrier, rather than treating electrical and thermal systems independently.

5.3.2. Economic Performance and Net Profitability

Table 5 summarizes the economic results of Scenario S3. The annual revenue from electricity export amounts to 12.65×10^9 IRR, whereas the annualized cost associated with PV investment and operation (including capital recovery and maintenance) is 4.63×10^9 IRR. On the cost side, electricity purchased from the grid is reduced compared with Scenario S1 due to the elimination of electrically supplied furnace heating. Thermal energy costs increase slightly because the full heating demand is now covered by natural gas; however, this increase is more than compensated by the reduction in electricity expenditure and the substantial PV export revenue.

After accounting for all electricity and natural gas costs, as well as PV investment and operation expenses, Scenario S3 yields a strongly positive net annual energy balance of approximately 2.9×10^9 IRR/year. In other words, revenues from PV electricity export not only offset the total energy supply cost of the production facility but also generate a significant net profit. This result is primarily driven by the large differential between the feed-in tariff for solar electricity and the industrial electricity purchase tariff, combined with the economic advantage of gas-based thermal supply.

5.3.3. Environmental Impact

From an environmental perspective, Scenario S3 results in a reallocation of emission sources between electricity and thermal subsystems, accompanied by a moderate reduction in total on-site CO_2 emissions. Based on the optimization results, the total annual CO_2 emissions of the production facility in this scenario amount to 627,164 kg CO_2/year. Of this total, 321,408 kg CO_2/year originate from grid electricity consumption, corresponding exclusively to motor-driven electrical loads. The remaining emissions are associated with natural gas combustion in the hot-air furnaces, which now supply the entire thermal demand due to the economic advantage of gas-based heating over electrically assisted heating. Compared with the baseline scenario, emissions from electricity consumption are reduced as a direct consequence of eliminating electric furnace heating. However, this reduction is partially offset by an increase in natural gas consumption, as thermal demand is fully shifted to the gas-fired subsystem. The net effect is a moderate decrease in total plant-level CO_2 emissions, indicating that the primary benefit of Scenario S3 remains economic rather than environmental.

It should be emphasized that photovoltaic electricity generation is assumed to have zero operational emissions. Since all PV output is exported to the grid, the associated emission reductions occur outside the system boundary of the production facility and are therefore not credited to direct on-site emission mitigation. Nevertheless, at the power-system level, exported PV electricity contributes indirectly to decarbonization by displacing grid-based generation, representing an additional system-wide environmental benefit beyond the scope of plant-level accounting.

5.3.4. Discussion and Practical Implications

Scenario S3 illustrates that, under favorable feed-in tariff schemes, economic optimization may prioritize revenue maximization through electricity export rather than on-site renewable self-consumption. Importantly, the results also demonstrate the value of integrated energy-hub modeling: by allowing electricity and thermal demands to interact through cost signals, the model identifies a configuration in which gas-fired heating and grid electricity jointly minimize operating costs while PV generation functions as an independent revenue stream.

This finding should be interpreted as a policy-sensitive upper-bound economic scenario, rather than a universally optimal operational strategy. Practical deployment may be constrained by regulatory limits on export capacity, grid interconnection agreements, or future tariff revisions. Nonetheless, Scenario S3 highlights the strong incentive for industrial facilities to participate in renewable energy markets when supportive policy frameworks are in place.

Table 5. Economic and Environmental Results of Scenario S3 (PV Export-Oriented Configuration)

Parameter	Value	Unit
Installed PV capacity	250	kW
Annual PV electricity exported	401,500	kWh/year

10.22060/EEJ.2026.25913.6025

Annual PV export revenue	12,647,250,000	IRR/year
Annualized PV investment & O&M cost	4,625,000,000	IRR/year
Annual grid electricity	345,600	kWh/year
Annual electricity purchase cost	3,449,779,200	IRR/year
Annual natural gas cost	Same as S2	IRR/year
Net annual energy balance	**+2,859,947,124**	IRR/year
On-site CO_2 emissions	627,164	kg CO_2/year
Energy system role	Net electricity exporter	-

5.4. Role of Diesel Generation as a Backup Option

Scenario S4 evaluates the role of diesel generation as a reliability-oriented backup option under grid electricity uncertainty. Based on historical operational records of the studied facility, grid outages amount to approximately 120 hours per year, predominantly occurring during summer peak-demand periods. These interruptions impose significant operational risks on continuous production lines, where electricity supply is essential for motor-driven equipment and process continuity.

When grid uncertainty is incorporated into the baseline configuration without any backup generation, the system experiences forced production shutdowns during outage periods. In this case, electrical loads cannot be supplied, leading to production losses modeled through a lost-load penalty cost. As reported in Table 7, the inclusion of outage-related production loss increases the total annual system cost dramatically to 1.57×10^{10} IRR/year, despite only a marginal reduction in purchased grid electricity. It is important to note that, during outage periods, natural gas consumption remains essentially unchanged relative to the baseline scenario without uncertainty. This is because gas-fired furnaces continue operating at minimum levels to preserve thermal stability and avoid excessive cooling, which would otherwise increase restart time and operational stress after grid restoration. Consequently, the sharp cost increase in this scenario is driven almost entirely by lost production rather than by changes in energy procurement.

To mitigate outage-related losses, a diesel generator with a rated capacity of 90 kW is introduced as a backup power source. The diesel unit is explicitly modeled to supply only the critical electrical loads associated with motor-driven equipment, whose aggregated demand does not exceed the generator's rated capacity. In contrast, electrical heating previously used for furnace operation in the baseline scenario is fully replaced by natural gas in both diesel-integrated cases (S4-1 and S4-2). This shift is economically rational, as gas-based heating remains significantly cheaper than both diesel-generated electricity and grid electricity. As a result, during both normal and outage conditions, Diesel generation supplies only essential electrical loads and All thermal demand of the furnaces is met by natural gas. As summarized in Table 7, diesel generation supplies only 10,620 kWh/year, corresponding to approximately 3.07% of total annual electrical demand. This confirms that the generator operates exclusively during outage periods and remains inactive when grid electricity is available due to its higher marginal cost. Despite the relatively small energy contribution, the economic impact of diesel integration is substantial. The annualized diesel investment and operating cost amounts to 1.22×10^9 IRR/year; however, this cost is more than offset by the complete elimination of lost-load penalties. Consequently, the total annual system cost is reduced to 6.37×10^9 IRR/year, representing a reduction of nearly 60% compared to the outage-affected baseline without backup.

The results of Scenario S4 clearly demonstrate that diesel generation is not economically competitive as a primary energy source, but provides significant value as a reliability and risk-mitigation measure. Even limited diesel operation, covering only critical electrical loads during grid outages, yields substantial economic benefits by preventing extreme production losses. More importantly, this scenario highlights the necessity of explicitly incorporating grid reliability and lost-load costs into industrial energy hub optimization frameworks. In regions where electricity interruptions are non-negligible, ignoring reliability considerations can lead to severely underestimated system costs and misleading technology rankings. The findings confirm that resilience-oriented investments, although rarely optimal from a pure energy-cost perspective, can become economically indispensable once production continuity is properly valued.

Table 7. Comparison of baseline operation and diesel-integrated scenario (S4)

Parameter	S1: Baseline	S1: Baseline	S4-1: Grid + diesel	S4-2: Grid + diesel

		(considering grid uncertainty)		**(considering grid uncertainty)**
Diesel rated capacity (kW)	0	0	0	90
Annual grid electricity (kWh/year)	530,570	514,010	345,600	334,980
Annual Diesel generation (kWh/year)	0	0	0	10,620
Diesel share	0%	0%	0%	3.07%
Annualized diesel cost (IRR/year)	0	0	0	1.22×10^9
Annual electricity cost (IRR/year)	5.3×10^9	5.13×10^9	3.45×10^9	3.34×10^9
Annual natural gas cost (IRR/year)	1.53×10^9	1.58×10^9	1.71×10^9	1.71×10^9
Product decrease cost (IRR/year)	0	9.5×10^9	0	0
Total annual energy cost (IRR/year)	6.82×10^9	1.57×10^{10}	5.16×10^9	6.37×10^9

5.5. Contribution of Waste-Heat Recovery from Furnaces

Scenario S5 investigates the potential of waste heat recovery (WHR) from the hot-air furnace exhaust as a means of reducing natural gas consumption and associated emissions. Two sub-cases are examined. In the first case (S5-1), WHR is evaluated purely on an economic basis. Due to the relatively low natural gas tariff and the additional investment and maintenance costs of heat recovery equipment, the optimization does not select WHR, resulting in identical performance to the scenario S4-1. This outcome indicates that, under current fuel price conditions, the marginal fuel savings achievable through WHR are insufficient to offset the annualized investment and O&M costs of the recovery system. Consequently, WHR is not economically competitive when cost minimization is the sole objective.

In the second case (S5-2), WHR is assessed from an environmental perspective. As shown in Table 8, under this configuration, natural gas consumption is reduced by approximately 21%, leading to a decrease in CO_2 emissions from natural gas combustion from 272,586 kg/year to 240,830 kg/year. Consequently, total annual CO_2 emissions are reduced by 22.27% compared to the baseline. However, this environmental benefit comes at the expense of a higher total annual cost (compared with scenario S5-1), primarily due to the annualized investment and O&M costs of the WHR system.

These results indicate that, under current fuel price structures, WHR is more appropriately justified as an emission mitigation measure rather than a cost-minimization strategy. This trade-off is particularly relevant for policy-driven decarbonization efforts in thermal-intensive industrial processes.

Table 8. Comparison of baseline operation and WHR-integrated scenario (S5)

Parameter	**S1: Baseline**	**S5-1: WHR (Economical)**	**S5-2: WHR (Environmental)**
Annual natural gas consumption (m^3/year)	129,803	145,598	114,681
Annualized investment & O&M cost of WHR (IRR/year)	-	-	608,300,000
Annual thermal energy cost (IRR/year)	1,526,739,970	1,712,523,676	1,348,877,922
Gas consumption reduction due to WHR	0%	0%	21.23%
Total annual energy cost (IRR/year)	6.82×10^9	5.16×10^9	5.41×10^9
CO_2 from natural gas (kg CO_2/year)	272,586	305,756	240,830
Total CO_2 emissions (kg CO_2/year)	766,016	660,334	595,408
CO_2 reduction vs. S1	-	13.79%	22.27%

5.6. Comparative Scenario Analysis

To provide a holistic assessment of the proposed energy hub configurations, two comprehensive optimization scenarios are evaluated, each reflecting a distinct strategic objective:

- S6: Joint optimization of all available energy supply options with the objective of total cost minimization.
- S7: Joint optimization of all available energy supply options with the objective of total CO_2 emission minimization.

These scenarios represent the extreme ends of the economic–environmental trade-off spectrum and serve as decision-support benchmarks for industrial energy planning.

5.6.1. Cost-Oriented Integrated Optimization (Scenario S6)

The optimization outcomes of Scenario S6 are fully aligned with those obtained in Scenario S3. When the objective function is defined solely in terms of economic performance, the model prioritizes configurations that maximize net financial benefit. Under the assumed tariff structure (characterized by a high photovoltaic feed-in tariff relative to the industrial electricity purchase price) the optimization naturally converges toward maximizing PV electricity export.

As a result, Scenario S6 selects:

- the maximum installable PV capacity,
- full export of PV-generated electricity to the grid,
- continued reliance on grid electricity and natural gas for internal energy demands.

This behavior confirms that Scenario S3 represents the globally cost-optimal solution among all evaluated configurations. Therefore, Scenario S6 does not introduce a new operational regime but rather validates the robustness of the PV export-oriented strategy under unconstrained cost minimization.

5.6.2. Emission-Oriented Integrated Optimization (Scenario S7)

Scenario S7 explores the system configuration that minimizes total CO_2 emissions by simultaneously activating all available low-carbon and efficiency-enhancing technologies. As summarized in Table 8, this scenario integrates:

- maximum photovoltaic capacity (250 kW),
- waste heat recovery in its environmentally optimal configuration,
- minimized reliance on grid electricity,
- reduced natural gas consumption.

Compared to the baseline scenario (S1), annual grid electricity consumption is reduced from 530,570 kWh/year to 94,531 kWh/year, while annual natural gas consumption decreases from 129,803 m³/year to 102,240 m³/year. These reductions result in a substantial decrease in CO_2 emissions from both energy carriers. Total annual CO_2 emissions are reduced from 766,016 kg CO_2 /year in S1 to 302,618 kg CO_2 /year in S7, corresponding to a 60.49% reduction. This significant improvement highlights the strong decarbonization potential of coordinated renewable integration and thermal efficiency enhancement within an industrial EH. From an economic perspective, the total annual energy cost in Scenario S7, excluding PV export revenue, amounts to 5.57×10^9 IRR/year, which remains higher than the minimum-cost solution. However, when revenues from PV electricity export are included, the net annual energy cost is dramatically reduced to 8.3×10^8 IRR/year. It should be emphasized that this economic benefit is a secondary outcome, as the primary objective of Scenario S7 is emission minimization rather than cost reduction.

Table 8. Comparison of baseline operation and scenario S7

Parameter	S1	S7
Annual grid electricity (kWh/year)	530,570	94,531
Annual natural gas consumption (m³/year)	129,803	102,240
Installed PV capacity (kW)	-	250
Annual PV electricity exported (kWh/year)	-	150,431
Annualized PV investment & O&M cost	-	4,625,000,000
Annual PV export revenue (IRR/year)	-	4,738,576,500
Gas consumption reduction due to WHR	-	21
CO_2 from electricity (kg CO_2/year)	493,430	87,914
CO_2 from natural gas (kg CO_2/year)	272,586	214,704
Total CO_2 emissions estimate (kg CO_2/year)	**766,016**	**302,618**

10.22060/EEJ.2026.25913.6025

CO_2 reduction vs. S1	-	60.49%
Total annual energy cost without PV revenue (IRR/year)	**6,822,889,710**	**5,568,608,442**
Total annual energy cost with PV revenue (IRR/year)	**6,822,889,710**	**830,031,942**

The comparative analysis of Scenarios S6 and S7 reveals a clear trade-off between economic optimality and environmental performance. While Scenario S6 (equivalent to S3) delivers the lowest total cost due to favorable electricity market conditions, Scenario S7 achieves the most substantial reduction in CO_2 emissions through aggressive deployment of renewable generation and efficiency measures.

The choice between these scenarios ultimately depends on strategic priorities, regulatory constraints, and sustainability targets. In regions with strong renewable support mechanisms, Scenario S6 may represent an economically dominant solution. Conversely, in policy frameworks emphasizing decarbonization, Scenario S7 provides a technically feasible and highly effective pathway toward significant emission reduction in thermal-intensive industrial processes.

5.7. Sensitivity and Economic Robustness Analysis

Since the optimal scheduling results are inherently influenced by techno-economic assumptions, a comprehensive sensitivity analysis was conducted to evaluate the robustness of the proposed Energy Hub formulation under different market and regulatory conditions. In particular, the impacts of the photovoltaic (PV) feed-in tariff, electricity purchase tariff, natural gas price, and investment costs of the PV and waste heat recovery (WHR) systems were systematically investigated. The selected parameters represent the primary economic drivers affecting industrial energy management decisions and are subject to significant regional and temporal variations. The objective of this analysis is not only to assess the stability of the obtained optimal solutions but also to identify the economic conditions under which different energy supply strategies become preferable.

For each sensitivity case, only one economic parameter was varied while all remaining technical and economic parameters were maintained at their baseline values. This one-factor-at-a-time approach enables the individual influence of each parameter on the optimal solution to be quantified without introducing confounding interactions. The optimization model was solved repeatedly using the same linear programming formulation, thereby ensuring that any variation in the objective function or energy dispatch originated solely from the investigated parameter. The results provide valuable insights into the economic resilience of the proposed Energy Hub and improve the practical applicability of the proposed framework under evolving market conditions.

5.7.1. Sensitivity to Feed-in Tariff

The feed-in tariff (FIT) is one of the most influential regulatory parameters affecting the economic performance of grid-connected photovoltaic systems. To evaluate the robustness of the proposed Energy Hub under different policy conditions, the PV export tariff was varied from 25% to 125% of the baseline value while maintaining all other technical and economic parameters unchanged. For each tariff level, the linear programming model was solved independently, and the resulting operating cost, grid electricity purchase, PV generation, and export revenue were recorded.

As illustrated in Fig. 4 (a), the objective function decreases almost linearly as the feed-in tariff increases. This behaviour is expected because higher export incentives directly increase the economic value of photovoltaic generation without altering the underlying technical constraints of the optimization problem. Within the investigated range, the operating cost continuously declines and eventually becomes negative at approximately 75% of the baseline tariff, indicating that the revenue obtained from electricity export is sufficient to fully offset the operating costs of the Energy Hub. Consequently, additional increases in the export tariff further improve the overall economic performance by generating net operational profit rather than merely reducing energy expenditure. A more detailed examination of the dispatch results (Fig. 4(b)) reveals that the optimal operating strategy exhibits only limited sensitivity to the feed-in tariff after a certain threshold. Both the purchased grid electricity and the utilized photovoltaic generation rapidly converge to nearly constant values once the tariff reaches approximately 50% of its reference value. This observation indicates that the available photovoltaic capacity becomes fully utilized under these conditions, and further increases in the export tariff primarily improve the economic return of exported electricity instead of changing the optimal energy dispatch.

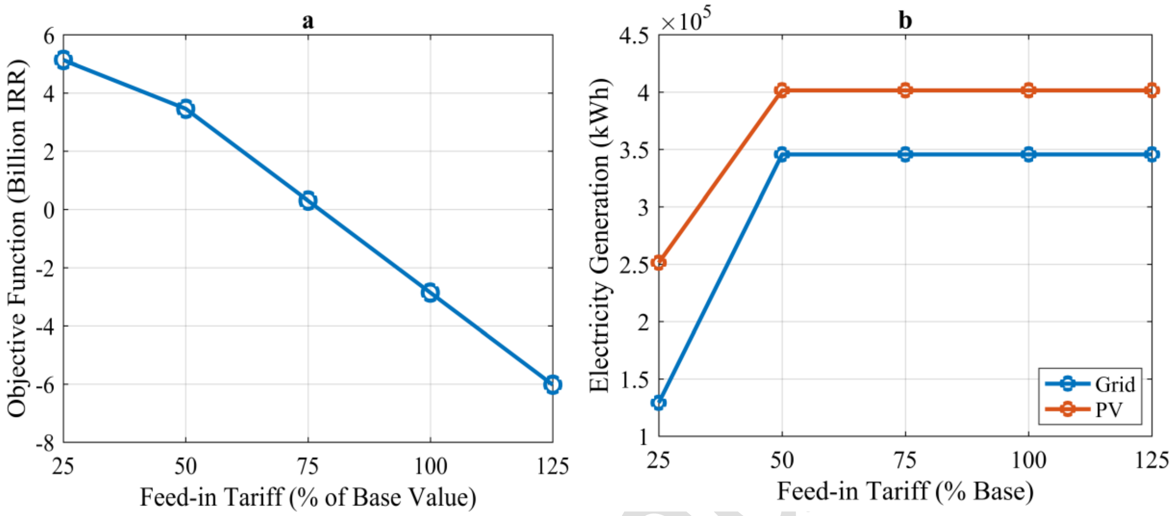

Fig. 4. Sensitivity to feed-in tariff: (a) Annual operating cost; (b) Optimal energy dispatch.

These findings demonstrate that the proposed optimization framework is economically robust over a wide range of feed-in tariff values. More importantly, they indicate that the superior economic performance of the PV-export scenario is not solely a consequence of the baseline tariff assumption adopted in this study. Instead, the proposed Energy Hub maintains its economic competitiveness under diverse regulatory environments, thereby enhancing the practical applicability of the proposed scheduling framework for industrial facilities operating under evolving electricity market policies. From a policy perspective, the results suggest that feed-in tariff mechanisms primarily influence the economic profitability of industrial photovoltaic investments rather than their operational scheduling once the installed PV capacity is fully utilized. Therefore, increasing export incentives beyond the identified threshold may improve investors' financial returns, but it is unlikely to produce substantial additional reductions in grid electricity consumption or significant changes in operational behaviour. This finding provides useful guidance for regulators seeking to balance renewable energy incentives with market efficiency while avoiding excessive subsidy levels.

5.7.2. Sensitivity to Electricity Purchase Tariff

The electricity purchase tariff represents one of the principal operating cost components in industrial energy hubs. To investigate its influence on the proposed optimization framework, the grid electricity price was varied between 50% and 150% of its baseline value while maintaining all remaining technical and economic parameters unchanged. For each tariff level, the linear programming model was re-optimized, and the corresponding operating cost and optimal energy dispatch were recorded.

As illustrated in Fig. 5(a), the total operating cost increases monotonically with the electricity purchase tariff. However, the relationship is not perfectly linear over the investigated range. A relatively sharp increase in operating cost is observed as the tariff approaches its baseline value, whereas the rate of increase becomes noticeably smaller for higher tariff levels. This behaviour indicates that the optimization gradually exploits the available photovoltaic generation to mitigate the impact of

10.22060/EEJ.2026.25913.6025

increasing electricity prices. Once the photovoltaic resource reaches its operational limit, further tariff increases primarily affect the operating cost rather than the optimal dispatch strategy. The corresponding dispatch results are presented in Fig. 5(b). At low electricity tariffs (approximately 50-75% of the baseline value), electricity demand is supplied predominantly from the grid, while photovoltaic generation remains economically unattractive. As the electricity tariff increases, a distinct transition occurs in the optimal scheduling strategy. Around 100% of the baseline tariff, photovoltaic generation becomes economically competitive, resulting in a substantial increase in PV utilization and a corresponding reduction in the reliance on grid electricity. Beyond this transition region, both the purchased grid electricity and photovoltaic generation converge towards nearly constant values, indicating that the installed PV capacity is fully utilized and additional tariff increases no longer produce significant changes in the dispatch solution.

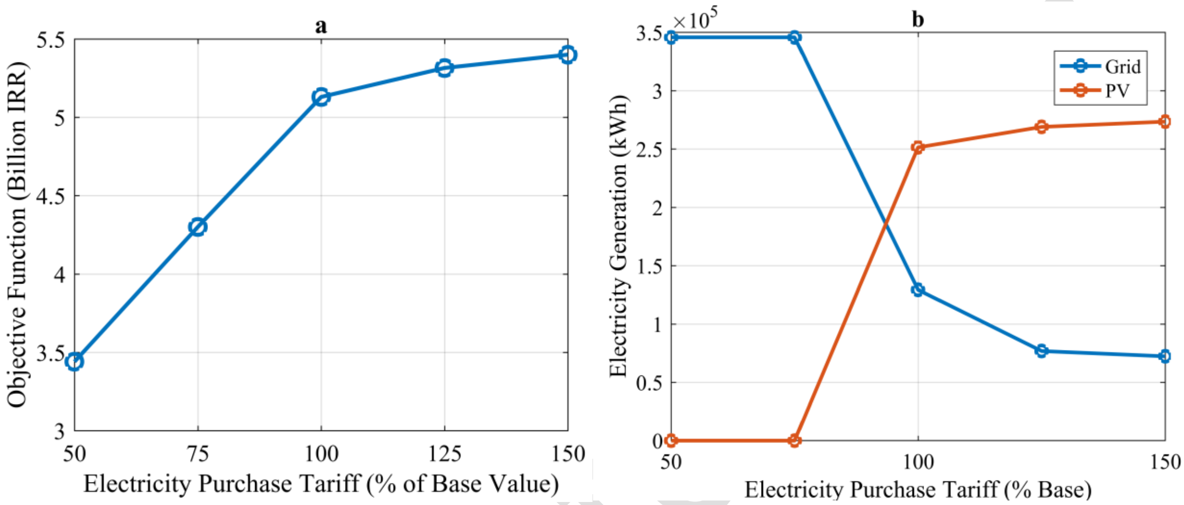

Fig. 5. Sensitivity to electricity purchase tariff: (a) Annual operating cost; (b) Optimal energy dispatch.

These results demonstrate that the proposed Energy Hub exhibits strong adaptability to changing electricity market conditions. More importantly, the analysis identifies a clear economic switching point beyond which further increases in electricity tariffs mainly influence operating expenditures rather than the optimal operating strategy. This finding provides practical guidance for industrial decision-makers by highlighting the tariff conditions under which photovoltaic integration becomes economically justified and when additional increases in electricity prices no longer result in meaningful operational changes.

5.7.3. Sensitivity to Natural Gas Price

Natural gas constitutes the primary fuel supplying the thermal demand of the industrial curing furnace and therefore represents one of the most influential economic parameters in the proposed Energy Hub. To assess the robustness of the optimization framework, the natural gas price was varied from 100% to 400% of its baseline value while maintaining all remaining technical and economic parameters unchanged. Figure 6(a) illustrates the influence of natural gas price on the annual operating cost. As expected, the operating cost increases almost linearly with increasing fuel price because natural gas remains the dominant thermal energy source throughout the investigated operating range. The nearly linear trend also confirms that the proposed linear programming formulation provides a stable and predictable response to fuel price variations without introducing abrupt changes in the optimization process. The corresponding electricity dispatch is presented in Fig. 6(b). The results indicate that the optimal utilization of photovoltaic generation remains nearly unchanged over the investigated gas price range, suggesting that photovoltaic operation is primarily governed by electricity-related economic factors rather than natural gas pricing. In contrast, the amount of purchased grid electricity exhibits a noticeable increase when the gas price exceeds approximately 300% of the baseline value, indicating a

10.22060/EEJ.2026.25913.6025

transition in the optimal operating strategy under extreme fuel price conditions. A more detailed assessment of the thermal subsystem is provided in Fig. 6(c). As natural gas prices increase, total natural gas consumption decreases considerably, while the contribution of the waste heat recovery (WHR) system increases rapidly from zero to approximately 21% of the furnace thermal demand. Beyond approximately 150% of the baseline gas price, the recovered heat contribution reaches a nearly constant level, indicating that the available recoverable waste heat has been fully exploited. Consequently, further increases in fuel price cannot produce additional reductions in gas consumption through WHR because the technical recovery potential has already been exhausted.

Overall, these results demonstrate that increasing natural gas prices substantially improve the economic attractiveness of WHR technologies. However, the analysis also reveals the existence of a practical recovery limit imposed by the available exhaust heat rather than by economic considerations alone. This finding highlights the importance of simultaneously considering both economic and thermodynamic constraints when evaluating industrial WHR systems.

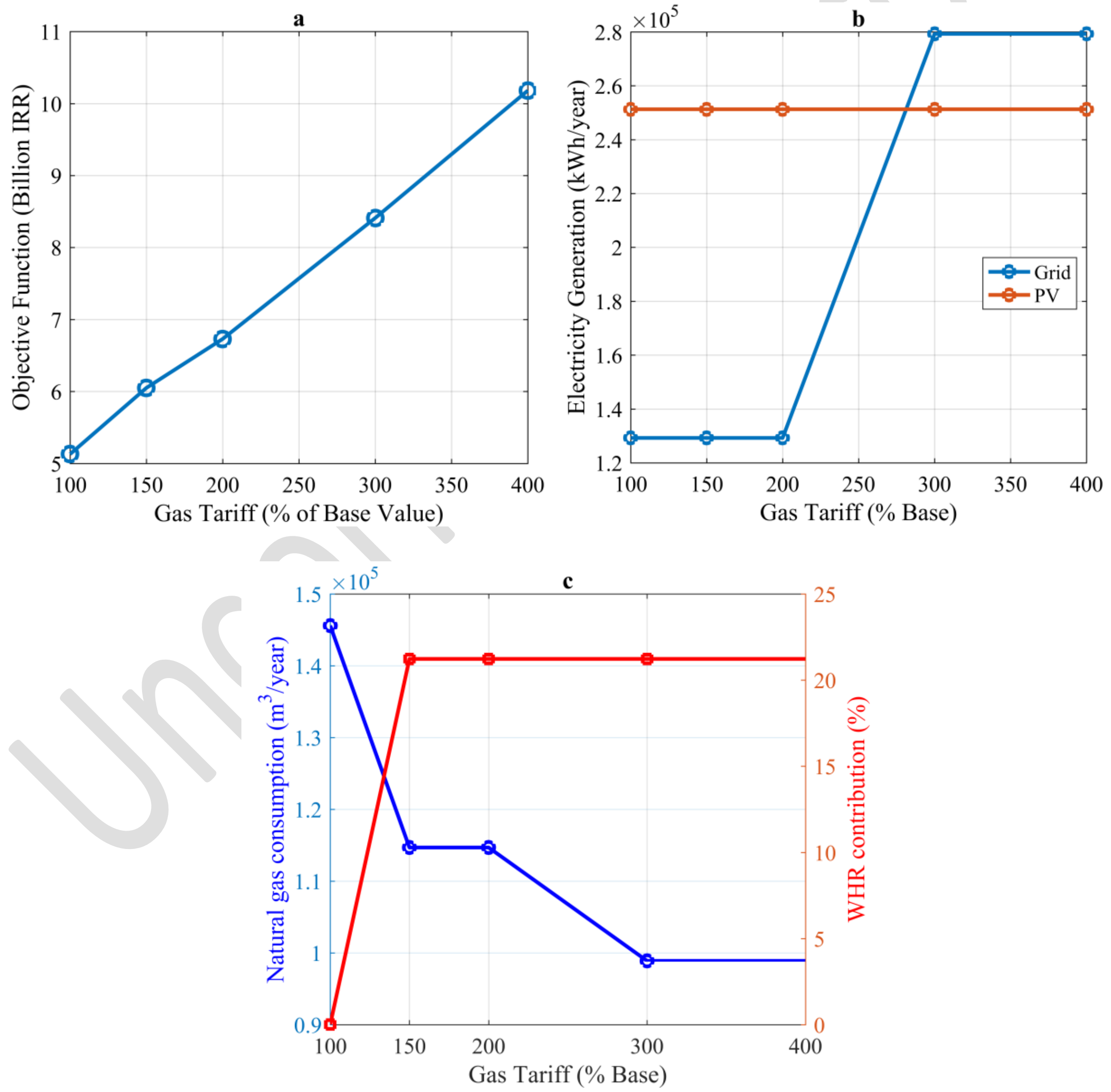

Fig. 6. Sensitivity to Gas tariff: (a) Annual operating cost; (b) Optimal electrical energy dispatch; and (c) Optimal thermal energy dispatch

5.7.4. Sensitivity to PV and WHR Capital Cost

Capital investment represents one of the most influential factors affecting the long-term economic feasibility of distributed energy technologies. To evaluate the robustness of the proposed Energy Hub against investment uncertainty, separate sensitivity analyses were performed for the capital costs of the photovoltaic (PV) system and the waste heat recovery (WHR) unit while maintaining all other technical and economic parameters at their baseline values.

A. PV Capital Cost

The results obtained for the PV investment cost are presented in Fig. 7. As shown in Fig. 7(a), the annual operating cost increases as the photovoltaic capital cost rises. However, the increase is nonlinear and gradually approaches a plateau at higher investment levels. This behaviour indicates that the optimization progressively reduces the economic attractiveness of photovoltaic generation as the investment cost increases.

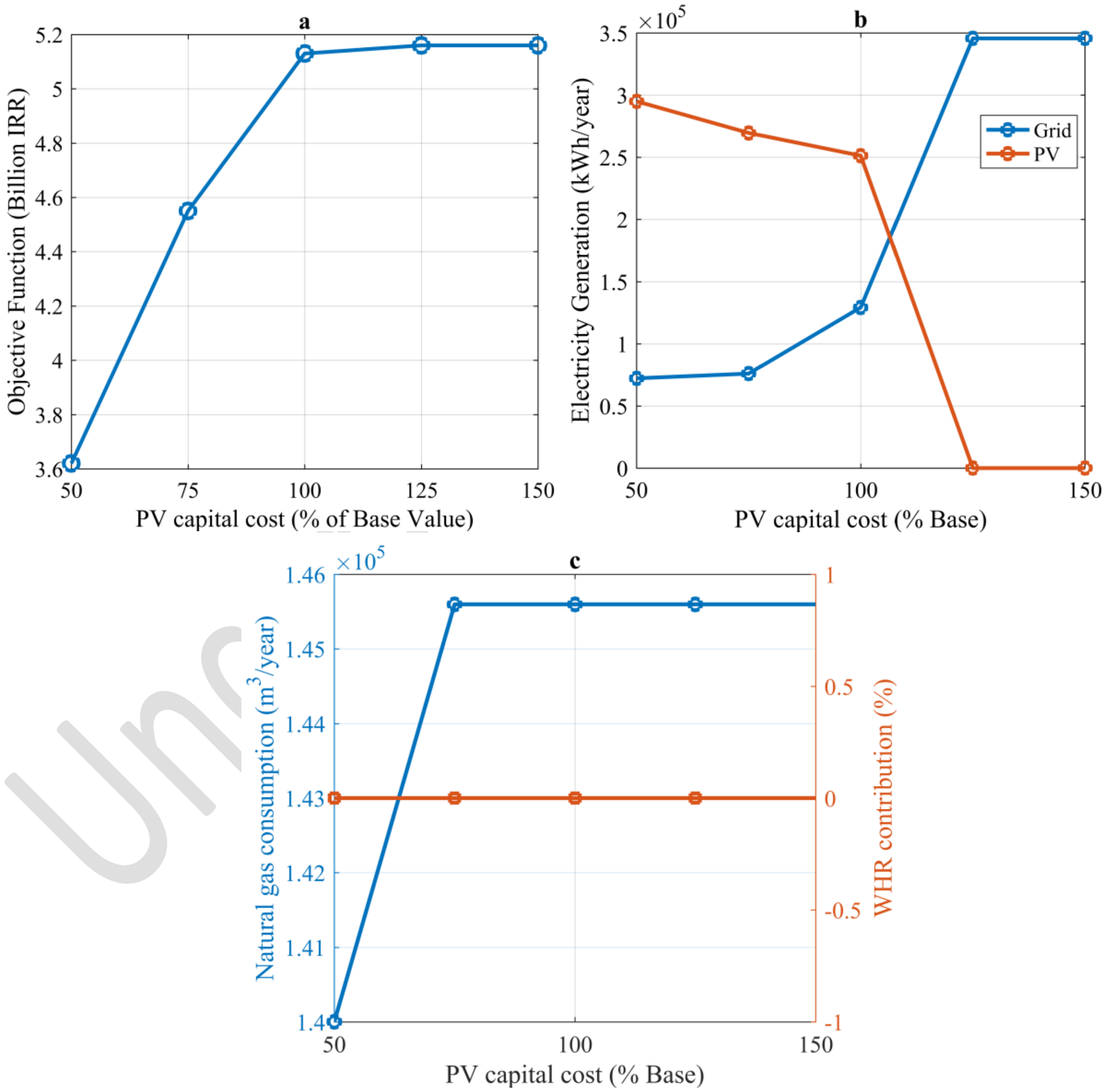

Fig. 7. Sensitivity to PV capital cost: (a) Annual operating cost; (b) Optimal electrical energy dispatch; and (c) Optimal thermal energy dispatch

10.22060/EEJ.2026.25913.6025

The corresponding dispatch results are illustrated in Fig. 7(b). When the photovoltaic capital cost remains below the baseline value, photovoltaic generation supplies a substantial portion of the electrical demand, significantly reducing the dependence on grid electricity. As the capital cost exceeds approximately 125% of the reference value, photovoltaic generation is almost completely excluded from the optimal solution, and the electrical demand is predominantly supplied by the utility grid. This transition identifies an economic investment threshold beyond which additional photovoltaic deployment is no longer financially justified under the assumed market conditions.

The thermal dispatch presented in Fig. 7(c) confirms that variations in photovoltaic investment cost have only a negligible influence on the thermal subsystem. Natural gas consumption changes only marginally, while the contribution of the waste heat recovery system remains essentially unchanged. This behaviour demonstrates the weak coupling between photovoltaic investment decisions and thermal energy management within the proposed industrial Energy Hub.

B. WHR Capital Cost

The influence of WHR investment cost is illustrated in Fig. 8. Unlike photovoltaic investment, variations in WHR capital cost produce only a relatively small increase in the annual operating cost, as shown in Fig. 8(a). This observation suggests that WHR contributes to operational savings primarily through fuel conservation rather than through significant reductions in total operating expenditure.

The electrical dispatch remains virtually unchanged throughout the investigated investment range (Fig. 8(b)), indicating that modifications in WHR investment cost do not affect the optimal scheduling of electrical energy resources.

The thermal subsystem, however, exhibits a pronounced response (Fig. 8(c)). When the WHR capital cost is relatively low, recovered exhaust heat provides approximately 22% of the thermal demand, leading to a noticeable reduction in natural gas consumption. As the investment cost increases beyond approximately 75% of the baseline value, the optimization gradually excludes the WHR system from the optimal solution, resulting in a corresponding increase in natural gas consumption and the complete disappearance of waste heat utilization. This behaviour identifies a clear economic break-even region for WHR deployment under the assumed fuel price conditions.

Overall, the investment sensitivity analysis demonstrates that photovoltaic systems exhibit greater economic sensitivity to capital cost variations than WHR technologies. In contrast, WHR investment decisions are governed primarily by fuel cost savings and therefore become economically attractive only when the capital investment remains below a certain threshold.

10.22060/EEJ.2026.25913.6025

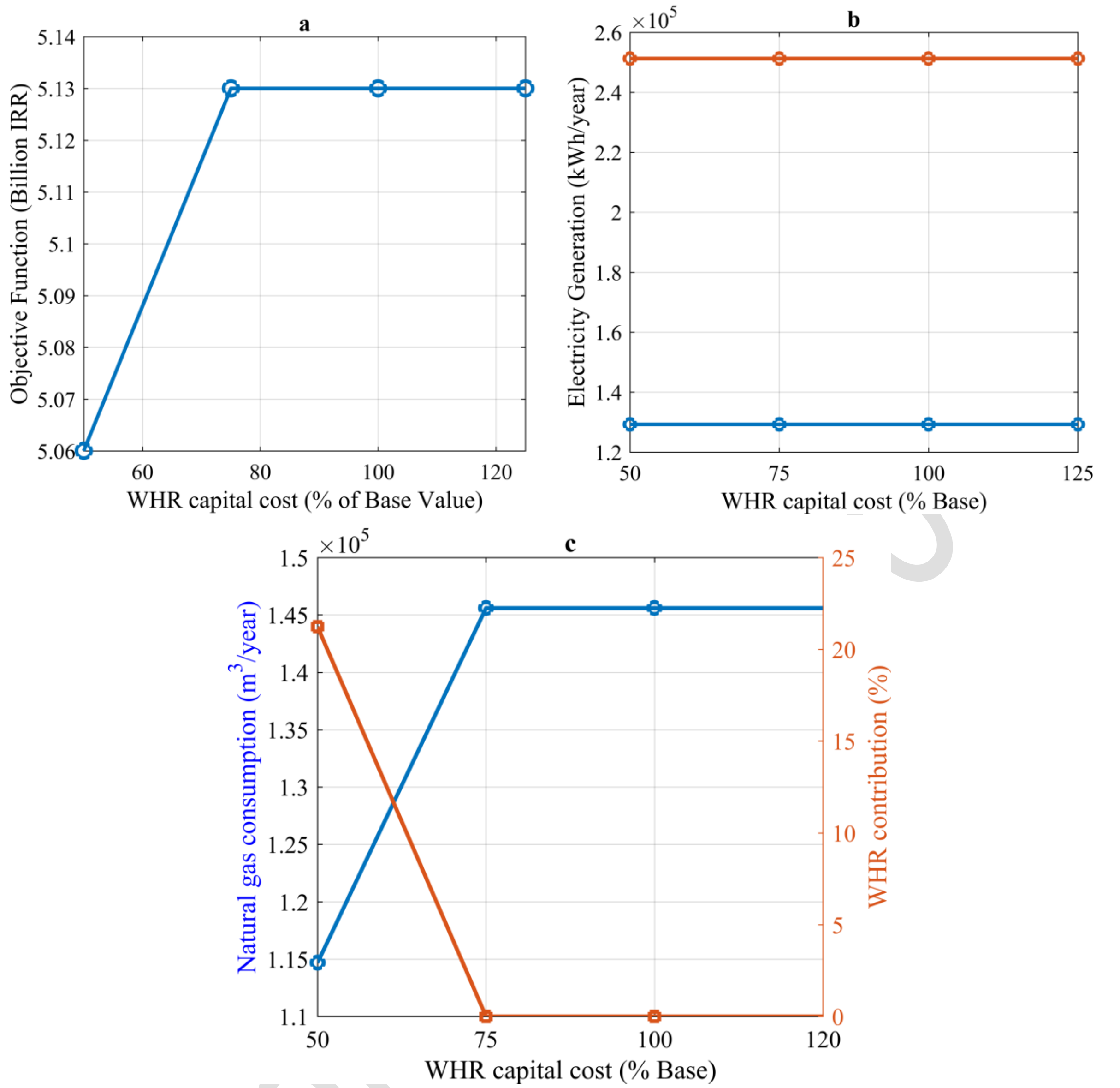

Fig. 8. Sensitivity to WHR capital cost: (a) Annual operating cost; (b) Optimal electrical energy dispatch; and (c) Optimal thermal energy dispatch

5.7.5. Economic Robustness, Break-even Analysis and Policy Implications

The sensitivity analyses presented in Sections **5.7.1–5.7.4** provide a comprehensive assessment of the economic robustness of the proposed Energy Hub under varying market and investment conditions. Although the annual operating cost changes in response to electricity tariffs, natural gas prices, feed-in tariffs, and capital investment assumptions, the optimization consistently converges toward economically rational operating strategies. This behavior indicates that the proposed LP-based Energy Hub formulation remains numerically stable and economically consistent over a wide range of realistic industrial operating conditions. The results further reveal that each economic parameter affects the Energy Hub through a different physical and economic mechanism. Feed-in tariffs mainly influence the economic value of photovoltaic electricity exports without significantly changing the optimal dispatch after the available PV capacity has been fully utilized. In contrast, increasing electricity purchase tariffs encourages greater reliance on local renewable generation and reduces grid dependency. Similarly,

AUT Journal of Electrical Engineering
10.22060/EEJ.2026.25913.6025

higher natural gas prices progressively improve the economic attractiveness of waste heat recovery by increasing the value of recovered thermal energy, although the achievable savings eventually become limited by the finite amount of recoverable exhaust heat. On the other hand, increases in the capital cost of PV or WHR technologies gradually reduce their economic competitiveness, defining practical investment thresholds beyond which conventional energy supply becomes economically preferable. To complement the operational optimization results, a simplified investment assessment was carried out using the annual operating cost savings obtained from the optimization model. Since the proposed formulation already annualizes the capital investment through the CRF described in Section 4.3.2, the annual economic benefits can be directly compared with the equivalent annualized investment cost. The Simple Payback Period (SPP) is therefore calculated as

$$SPP = \frac{C_{CAPEX}}{S_{annual}} \tag{25}$$

where C_{CAPEX} denotes the initial capital investment and S_{annual} represents the annual operating cost savings relative to the reference scenario. The SPP provides a straightforward indicator of investment attractiveness and allows comparison among different technology configurations. In addition, the long-term profitability of the investment was evaluated using the Net Present Value (NPV), defined as

$$NPV = -C_{CAPEX} + \sum_{t=1}^{N} \frac{S_{annual} - C_{O\&M}}{\left(1+r\right)^{t}} \tag{26}$$

denotes the annual operation and maintenance cost. A positive NPV indicates that the cumulative discounted savings exceed the initial investment cost, confirming the long-term economic feasibility of the proposed technology.

Table 9 summarizes the principal economic indicators for the investigated investment scenarios, including annual operating cost savings, Simple Payback Period, and Net Present Value. These indicators complement the operational optimization results by quantifying the financial attractiveness of the proposed Energy Hub from an industrial investment perspective.

Overall, the combined sensitivity and economic analyses indicate that photovoltaic deployment is primarily governed by electricity market policies and investment cost, whereas the viability of waste heat recovery depends mainly on fuel prices and the amount of recoverable exhaust heat. Consequently, industrial energy efficiency policies should not rely exclusively on electricity market incentives. Instead, balanced policy mechanisms (including stable feed-in tariffs, investment incentives for renewable generation, and financial support for industrial WHR technologies) can substantially improve the long-term economic performance of integrated industrial energy systems. The obtained results therefore provide practical guidance for plant operators, industrial investors, and policymakers when evaluating future investments under evolving energy market conditions.

Table 9. Economic feasibility indicators of the investigated investment scenarios.

Scenario	SPP (years)	NPV (IRR)
PV (S2)	6.47	4.15×10^{9}
WHR (S5)	8.35	-1.4×10^{9}
PV + WHR (S7)	4.92	6.22×10^{9}
PV exporting (S3)	4.35	6.82×10^{9}

As shown in Table 9, noticeable differences exist in the economic performance of the investigated technologies. The standalone photovoltaic system (Scenario S2) achieves a positive economic return with a Simple Payback Period of 6.47 years and a Net Present Value of 4.15×10^9 IRR, indicating that

10.22060/EEJ.2026.25913.6025

PV investment is economically feasible even under self-consumption operation. However, the PV exporting scenario (Scenario S3) exhibits the highest economic attractiveness, reducing the payback period to 4.35 years while increasing the NPV to 6.82×10^9 IRR. This result confirms that favorable feed-in tariffs substantially improve investment profitability by transforming photovoltaic generation from a load-reduction technology into a revenue-generating asset.

In contrast, the standalone waste heat recovery system (Scenario S5) presents the weakest economic performance, with a payback period of 8.35 years and a negative NPV (-1.40×10^9 IRR). Although the system reduces natural gas consumption and associated emissions, the current industrial natural gas tariff is insufficient to recover the initial investment within an economically attractive timeframe. This finding is fully consistent with the sensitivity analysis presented in Section 5.7.3, which demonstrated that increasing natural gas prices considerably improve the economic competitiveness of WHR systems. The combined PV–WHR configuration (Scenario S7) offers a balanced techno-economic solution, achieving a payback period of 4.92 years together with a positive NPV of 6.22×10^9 IRR. Although its economic return is slightly lower than that of the PV-export scenario, the integrated configuration simultaneously delivers renewable electricity generation, waste heat utilization, reduced natural gas consumption, and lower carbon emissions. Therefore, from a broader sustainability perspective, Scenario S7 represents an attractive compromise between economic profitability and industrial decarbonization.

Overall, the combined sensitivity and economic analyses indicate that photovoltaic deployment is primarily governed by electricity market policies and investment cost, whereas the viability of WHR depends mainly on fuel prices and the amount of recoverable exhaust heat. Consequently, industrial energy efficiency policies should not rely exclusively on electricity market incentives. Instead, balanced policy mechanisms (including stable feed-in tariffs, investment incentives for renewable generation, and financial support for industrial WHR technologies) can substantially improve the long-term economic performance of integrated industrial energy systems. The obtained results therefore provide practical guidance for plant operators, industrial investors, and policymakers when evaluating future investments under evolving energy market conditions.

5.8. Discussion and Practical Implications

The obtained results clearly demonstrate that the fabric-concrete production line constitutes a highly suitable candidate for EH-based optimization. The coexistence of steady electrical loads, continuous thermal demand, and recoverable furnace exhaust heat creates favorable conditions for coordinated multi-carrier energy management, where economic, environmental, and reliability objectives can be explicitly balanced within a unified framework.

From a practical perspective, the proposed EH model provides directly actionable insights for industrial decision-makers. The results quantitatively identify optimal PV sizing thresholds, clarify the limited economic role of diesel generators under normal operating conditions, and reveal the conditions under which waste-heat recovery becomes environmentally meaningful despite weak economic incentives. In particular, the analysis highlights that diesel generation should not be interpreted as a cost-competitive energy source, but rather as a resilience-oriented asset whose value emerges only when grid reliability and lost-load penalties are explicitly considered.

A key finding of this study is the dominant influence of regional energy tariff structures on optimal system configuration. High feed-in tariffs for exported electricity fundamentally alter the economic role of PV systems, shifting them from a self-consumption-oriented technology to a revenue-generating asset. Conversely, low natural gas prices substantially weaken the economic justification for WHR, even in thermal-intensive industrial processes. This asymmetry underscores the necessity of distinguishing between cost-driven, emission-driven, and reliability-driven technologies when designing industrial EHs.

The comprehensive sensitivity analyses presented in Section 5.7 further demonstrate the economic robustness of the proposed framework. Although the annual operating cost varies with electricity tariffs, natural gas prices, feed-in tariffs, and capital investment assumptions, the optimization consistently converges toward economically

10.22060/EEJ.2026.25913.6025

rational dispatch solutions. This stable behavior confirms that the proposed formulation remains applicable across a wide range of realistic industrial operating conditions and provides reliable support for industrial decision-making under different market scenarios.

To further evaluate the practical value of the proposed framework, Table 10 compares the present study with representative recent Energy Hub optimization studies reported in the literature. Unlike many recent studies that employ stochastic MILP, robust optimization, or distributed multi-agent approaches to address uncertainty, the proposed framework intentionally adopts a deterministic LP formulation to prioritize computational efficiency, transparency, and practical deployability in industrial environments. The model directly utilizes measured factory-scale operational data, explicitly incorporates furnace-level waste heat recovery, and can be solved with very low computational burden using a standard LP solver. Although advanced stochastic formulations generally provide greater robustness against uncertain renewable generation and volatile energy prices, they also introduce significantly higher computational complexity, larger optimization models, and increased data requirements that may reduce their suitability for routine industrial scheduling applications.

Accordingly, the primary contribution of this work should not be interpreted as the development of a new optimization algorithm. Instead, its contribution lies in demonstrating that a computationally efficient LP-based Energy Hub model, calibrated using measured industrial operating data and explicitly integrating furnace waste heat recovery, can achieve economically meaningful and practically implementable solutions for factory-scale multi-energy management. This application-oriented contribution distinguishes the present work from many existing studies that primarily emphasize methodological complexity while relying on synthetic case studies or benchmark systems.

Finally, the proposed framework also provides several policy-relevant insights. The results indicate that electricity tariff structures play a dominant role in determining the economic attractiveness of photovoltaic investments, whereas low natural gas prices substantially reduce the financial incentive for industrial waste heat recovery despite its environmental benefits. These findings suggest that balanced industrial energy policies (including stable renewable electricity incentives together with mechanisms supporting industrial waste heat utilization) may significantly improve the long-term economic performance of integrated industrial Energy Hubs while simultaneously contributing to energy efficiency and decarbonization objectives.

Table 10. Comparison of the proposed industrial energy hub framework with representative recent studies

Ref.	**Application domain**	**Energy carriers & technologies**	**Waste-heat recovery (WHR)**	**Optimization method**	**Uncertainty modeling**	**Field data used?**	**Computational burden**
[9]	NH_3-based CCHHP Energy Hub	Elec., Heat, H_2, NH_3, Cooling	×	Stochastic MILP	✓	×	High
[12]	Water–Energy Hub	Elec., Gas, Heat	×	MILP	×	×	Medium
[13]	IEGS / Microgrid	Elec., Gas	×	Two-stage stochastic	✓	×	High
[14]	CHHP EH	Elec., Heat, H_2	×	MILP	×	×	Medium
[15]	Multi-energy networks	Elec., Gas, Heat	×	Distributed optimization	×	×	High
[16]	Hydrogen EH	Elec., Heat, H_2	×	Stochastic MILP	✓	×	High
[17]	Multi-agent EH	Elec., Heat, RES	×	MILP	×	×	Medium
This paper	Factory-scale EH	Elec., Gas	✓	LP	×	✓	Very Low (<0.1sec.)

6. Conclusions and Future Work

10.22060/EEJ.2026.25913.6025

This paper presented an integrated EH framework for factory-scale energy optimization in a fabric-concrete production line characterized by continuous and tightly coupled electrical and thermal demands. By jointly modeling electricity, natural gas, photovoltaic generation, diesel backup, and furnace waste-heat recovery within a unified optimization structure, the proposed approach enables coordinated decision-making across multiple energy carriers under realistic operational constraints.

The results demonstrate that substantial reductions in annual energy cost and carbon emissions can be achieved through integrated electrical-thermal optimization. Photovoltaic integration effectively reduces grid dependency during production hours; however, its economic viability is shown to be strongly contingent on tariff design. Under low industrial electricity prices, PV self-consumption yields limited economic benefit, whereas favorable feed-in tariffs transform PV systems into dominant cost-reduction assets through electricity export. This finding highlights the decisive role of regulatory frameworks in shaping optimal industrial energy strategies. Sensitivity analyses confirmed that this conclusion remains robust over a broad range of tariff scenarios, highlighting the dominant role of regulatory policies in industrial energy investment decisions.

Waste-heat recovery exhibits a fundamentally different behavior. Although the proposed recuperative system consistently decreases natural gas consumption and associated carbon emissions, its economic competitiveness remains strongly dependent on fuel prices and investment costs. Under low natural gas tariffs, WHR is unlikely to be selected by purely cost-oriented optimization despite its environmental benefits. Consequently, wider industrial deployment of WHR technologies is likely to require supportive policy mechanisms such as carbon pricing, investment incentives, or dedicated energy-efficiency programs.

The proposed analyses also demonstrate that diesel generators should not be regarded as economically competitive primary energy sources under normal operating conditions. Instead, their value arises primarily from enhancing supply reliability and maintaining production continuity during grid outages. This finding reinforces the importance of explicitly distinguishing between cost-driven technologies, emission-reduction technologies, and resilience-oriented technologies when designing industrial Energy Hubs.

Beyond the specific case study, the proposed framework demonstrates the practical applicability of transparent LP-based optimization for factory-scale energy management. Compared with computationally intensive stochastic or mixed-integer optimization approaches, the deterministic LP formulation provides fast computation, straightforward implementation, and clear physical interpretability while preserving sufficient modeling fidelity for industrial techno-economic planning. These characteristics make the proposed methodology particularly suitable for rapid scenario evaluation and practical engineering decision support.

Nevertheless, several limitations should be acknowledged. The present study adopts a deterministic formulation and therefore does not explicitly represent uncertainties associated with renewable generation, future energy prices, or equipment failures. Moreover, the photovoltaic and waste heat recovery systems are evaluated as prospective investment options rather than existing plant installations. Consequently, the obtained results should be interpreted as a design-oriented techno-economic assessment under representative industrial operating conditions rather than a retrospective validation of historical plant operation.

Future research should extend the proposed framework by incorporating stochastic or robust optimization techniques to explicitly address renewable generation uncertainty, market price volatility, and grid reliability. The inclusion of electrical and thermal energy storage systems, demand response programs, long-term investment planning, dynamic electricity pricing, carbon pricing mechanisms, and equipment degradation models would further enhance the applicability of the proposed Energy Hub framework. In addition, future investigations may integrate life-cycle environmental assessment and multi-objective optimization to simultaneously evaluate economic performance, carbon emissions, and system resilience for sustainable industrial energy management.

Overall, this work demonstrates that EH-based optimization constitutes a systematic, scalable, and industry-oriented methodology for improving the economic and environmental performance of energy-intensive manufacturing facilities. The proposed framework bridges the gap between theoretical multi-energy optimization and practical industrial implementation by combining realistic plant operating conditions with a transparent and computationally efficient optimization model.

7. References

[1] JS, A., & Bhuvaneshwari, M. (2022). Textile-Reinforced Concrete Sandwich Panels: A Review. *ACI Structural Journal*, *119*(5).

[2] Imene, O. (2024). Techno-economic assessment of waste heat recovery systems in Nigerian manu-facturing industries.

[3] DoE, U. S. (2004). Waste Heat Reduction and Recovery for Improving Furnace Efficiency Productivity and Emissions Performance. *US Department of Energy: Washington, DC, USA*.

[4] Mancarella, P. (2014). MES (multi-energy systems): An overview of concepts and evaluation models. *Energy*, *65*, 1-17.

[5] Lasemi, M. A., Arabkoohsar, A., Hajizadeh, A., & Mohammadi-Ivatloo, B. (2022). A comprehensive review on optimization challenges of smart energy hubs under uncertainty factors. *Renewable and Sustainable Energy Reviews*, *160*, 112320.

[6] M. Azimi, A. Salami, M.S. Javadi, J.P. Catalão, Optimal and distributed energy management in interconnected energy hubs, *Appl. Energy* 365 (2024) 123282.

[7] S. Moradi, R. Ghaffarpour, A.M. Ranjbar, B. Mozaffari, Optimal integrated sizing and planning of hubs with midsize/large CHP units considering reliability of supply, *Energy Convers. Manag.* 148 (2017) 974–992.

[8] E. Shahrabi, S.M. Hakimi, A. Hasankhani, G. Derakhshan, B. Abdi, Developing optimal energy management of energy hub in the presence of stochastic renewable energy resources, *Sustain. Energy Grids Netw.* 26 (2021) 100428.

[9] Khanahmadi, A., Manthouri, M., & Ghaffarpour, R. (2025). Stochastic MILP-Based Optimization of an Ammonia-Fueled Energy Hub with Renewable Energy Uncertainty and Load Flexibility. Renewable Energy, 124999.

[10] A.A. Eladl, M.I. El-Afifi, M.M. El-Saadawi, B.E. Sedhom, Distributed optimal dispatch of smart multi-agent energy hubs based on consensus algorithm considering lossy communication network and uncertainty, *CSEE J. Power Energy Syst.* (2023).

[11] S.A. Ghappani, A. Karimi, Economic-environmental operation of a CHHP energy hub considering uncertainties and demand response programs, *IET Gener., Transm. Distrib.* 17 (19) (2023) 4399–4422.

[12] R. Ghaffarpour, A.M. Ranjbar, B. Mozaffari, Resilience oriented water and energy hub scheduling considering maintenance constraint, *Energy* (2018), doi: 10.1016/j.energy.2018.06.022.

[13] Z. Wei, P. Wei, C. Chen, H. Gao, Z. Luo, Y. Xiang, Two-stage stochastic decentralized low-carbon economic dispatch of integrated electricity-gas networks, *Energy* 282 (2023) 128325.

[14] S.A. Ghappani, A. Karimi, Optimal operation framework of an energy hub with combined heat, hydrogen, and power (CHHP) system based on ammonia, *Energy* 266 (2023) 126407.

[15] D. Xu, Q. Wu, B. Zhou, C. Li, L. Bai, S. Huang, Distributed multi-energy operation of coupled electricity, heating, and natural gas networks, *IEEE Trans. Sustain. Energy* 11 (4) (2019) 2457–2469.

[16] M. Agabalaye-Rahvar, A. Mansour-Saatloo, M.A. Mirzaei, B. Mohammadi-Ivatloo, K. Zare, Economic-environmental stochastic scheduling for hydrogen storage-based smart energy hub coordinated with integrated demand response program, *Int. J. Energy Res.* 45 (14) (2021) 20232–20257.

[17] S.A. Ghappani, A. Khanahmadi, R. Ghaffarpour, Consensus-based optimal operation of multi-agent renewable energy hubs considering various graph topologies, *Renewable Energy* 251 (2025) 123331.

[18] H. Jouhara, N. Khordehgah, S. Almahmmoud, B. Delpech, A. Chauhan, S.A. Tassou, Waste heat recovery technologies and applications, *Thermal Science and Engineering Progress* **6** (2018) 268–289.

[19] S. Sapali, P. Kittisupakorna, I.M. Mujtabab, A newly designed economizer to improve waste heat recovery: a case study in a pasteurized milk plant, *Appl. Thermal Eng.* **60** (1–2) (2013) 188–199.

[20] B. Delpech, B. Axcell, H. Jouhara, A review on waste heat recovery from exhaust in the ceramics industry, in: *International Conference on Advances in Energy Systems and Environmental Engineering (ASEE17)*, vol. 22, 2017.

[21] Eggleston, H. S., Buendia, L., Miwa, K., Ngara, T., & Tanabe, K. (2006). 2006 IPCC guidelines for national greenhouse gas inventories.